NAV-0215-FM-95046-940

UNIQUE FIBER OPTIC SENSOR SYSTEM FOR RESIDUAL STRESS MEASUREMENT ON GRAPHITE COMPOSITES

D. Bullock
Foster-Miller, Inc.
350 Second Avenue
Waltham, MA 02154-1196

December 1995

Final Report
Contract No. N00019-94-C-0215

Distribution Statement

"Approved for public release; distribution is unlimited. Disclosure outside the Government is subject to the restrictions of DFARS 227.405-79 (B) (1)."

Prepared for:

Naval Air Systems Command
Naval Air Systems Command Headquarters
1421 Jefferson Davis Highway
Arlington, VA 22243-5120

NAV-0215-FM-95046-940

UNIQUE FIBER OPTIC SENSOR SYSTEM FOR RESIDUAL STRESS MEASUREMENT ON GRAPHITE COMPOSITES

D. Bullock
Foster-Miller, Inc.
350 Second Avenue
Waltham, MA 02154-1196

December 1995

Final Report
Contract No. N00019-94-C-0215

Distribution Statement

Prepared for:

Naval Air Systems Command
Naval Air Systems Command Headquarters
1421 Jefferson Davis Highway
Arlington, VA 22243-5120

LICENSE RIGHTS LEGEND
Contract No. N00019-94-C-0215
Contractor or Subcontractor: Foster-Miller, Inc.

For a period of four (4) years after the delivery and acceptance of the last deliverable item under the above contract, this technical data shall be subject to the restrictions contained in the definition of "Limited Rights" in DFARS clause at 252.227-7013. After the four-year period, the data shall be subject to the restrictions contained in the definition of "Government Purpose License Rights" in DFARS clause 252.227-7013. The Government assumes no liability for unauthorized use or disclosure by others. This legend, together with the indications of the portions of the data which are subject to such limitations shall be included on any reproduction hereof which contains any portions subject to such limitations and shall be honored only as long as the data continues to meet the definition on Government purpose license rights.

REPORT DOCUMENTATION PAGE

Form Approved
OMB No. 0704-0188

1. AGENCY USE ONLY *(Leave blank)*	2. REPORT DATE	3. REPORT TYPE AND DATES COVERED
	December 1995	Final Report 11/22/94 to 9/30/95

4. TITLE AND SUBTITLE
Unique Fiber Optic Sensor System for Residual Stress Measurement on Graphite Composites

5. FUNDING NUMBERS
N00019-93-P6-MP038

6. AUTHOR(S)
D. Bullock

7. PERFORMING ORGANIZATION NAME(S) AND ADDRESS(ES)
Foster-Miller, Inc.
350 Second Avenue
Waltham, MA 02154-1196

8. PERFORMING ORGANIZATION REPORT NUMBER
NAV-0215-FM-95046-940

9. SPONSORING/MONITORING AGENCY NAME(S) AND ADDRESS(ES)
Naval Air Systems Command
Naval Air Systems Command Headquarters
1421 Jefferson Davis Highway
Arlington, VA 22243-5120

10. SPONSORING/MONITORING AGENCY REPORT NUMBER
N00019-94-C-0215

11. SUPPLEMENTARY NOTES
TPO: Mr. Thompson, AIR-5304C2

12a. DISTRIBUTION/AVAILABILITY STATEMENT
"Approved for public release; distribution is unlimited. Disclosure outside the Government is subject to the restrictions of DFARS 227.405-70 (B) (1)."

12b. DISTRIBUTION CODE
N/A

13. ABSTRACT *(Maximum 200 words)*

Virtually every composite fabrication process inherently results in the presence of residual strain in the component produced. Residual strain can result in warping and distortion of the finished part and seriously affect the component mechanical response to service loads. Measurement of this strain through the thickness of a composite is not a trivial task. Foster-Miller has developed the basis for a residual strain measurement system utilizing embedded fiber optic Bragg grating technology. Based on a novel tooling concept and advanced processing procedure, standard Bragg grating sensors were embedded through the thickness of flat plate and angled beam components and cured in place. Two conditions of residual strain were measured: strain due to thermal effects induced by the cure cycle and strain imparted into the composite by post-cure machining operations such as sectioning and drilling. It was proven that the embedded sensors could measure through-thickness tensile and compressive strain changes induced by various machining operations. It was also shown that residual strains due to thermal effects could be measured in high strain angled beams and that these strains correlated well to theoretical values predicted by finite element analysis.

14. SUBJECT TERM	15. NUMBER OF PAGES
sensors, composites, residual stress, fiber optic, cure, machining	38
	16. PRICE CODE: N/A

17. SECURITY CLASSIFICATION OF REPORT	18. SECURITY CLASSIFICATION OF THIS PAGE	19. SECURITY CLASSIFICATION OF ABSTRACT	20. LIMITATION OF ABSTRACT
Unclassified	Unclassified	Unclassified	Unlimited

CONTENTS

ILLUSTRATIONS

Figure **Page**

TABLES

1. INTRODUCTION

This final report describes work conducted by Foster-Miller for the U.S. Navy under Contract No. N00019-94-C-0215 as part of a Phase I SBIR program during the period November 22, 1994 through September 30, 1995. The objective of this program was to analytically and experimentally demonstrate the basis for a novel translaminar embedded fiber optic sensor system to directly measure residual strain through the thickness of components representative of advanced Navy aircraft composite structures. The approach to accomplishing this objective was to embed several Bragg grating sensors through the thickness of composite laminates of differing configurations. Two conditions of strain were measured: the residual strain due to thermal effects induced during the cure cycle as well as strain imparted into the composite structure by post-cure cycle machining operations such as cutting and drilling.

1.1 Bragg Grating Sensors

United Technologies Research Center (UTRC) has developed a method for exposing Bragg gratings into the core of optical fibers for use as strain sensors. A high intensity interference pattern created by superposed UV optical beams is impressed on a fiber to periodically modify inherent color centers in the core. Figure 1 shows the experimental setup for making the Bragg gratings in the optical fiber. *The gratings are made by imposing these periodic variations in the index of refraction along a short section in the core of the fiber,* typically 0.1 to 0.5 cm long. Figure 2 demonstrates how the grating provides an optical filter function for light propagating through its core with a very narrow bandwidth at a programmable wavelength. The gratings may be placed at will along the fiber for use as distributed, discrete gauge length sensors. *Because physical strain of the sensor causes a known shift in the wavelength of the filter function, each grating response can be measured and calibrated to provide direct strain measurements.* Time domain or wavelength domain multiplexing schemes can be utilized to interrogate each grating, independent from adjacent gratings.

A typical example of a fiber grating spectrum is shown in Figure 3. This spectral measurement is conducted by injecting broadband white light from a xenon arc lamp into a fiber with two sensor gratings, one of which is embedded in a composite. The reference sensor is not embedded in the composite material, so it provides a stable signal from which to interpret the shift in the response of the embedded device. The embedded sensor, about 2m from the reference sensor, is cured in the composite specimen with an orientation that was perpendicular to the plane of the specimen. A 1/2m grating spectrometer is used to accomplish the demultiplexing required to separate the responses of the reference and embedded sensors. The output of the spectrometer can be stored on hard disk using a general purpose computer-based analog/digital system. Figure 4 shows two different interrogation techniques. We will use the reflection technique since it requires access to only one side of the specimen which simplifies the fabrication process and limits complexity of the tooling.

This spectrum (Figure 3) provides an instantaneous "photograph" of the state of the sensor at any given time. Superimposing spectra as a function of time (or in this case, stress in the composite) results in a plot like Figure 5. This figure is generated by matching the reference grating peak for several spectra to show the shift of the embedded sensor peak as it is strained. A shift to the left indicates compression and a shift to the right indicates tension.

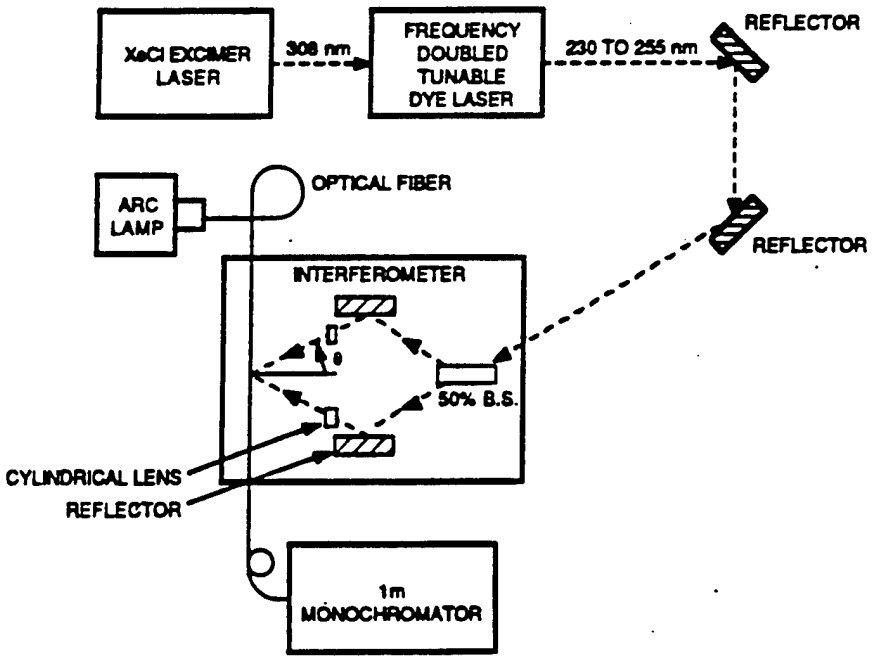

Figure 1. Experimental setup for making Bragg gratings in optical fibers

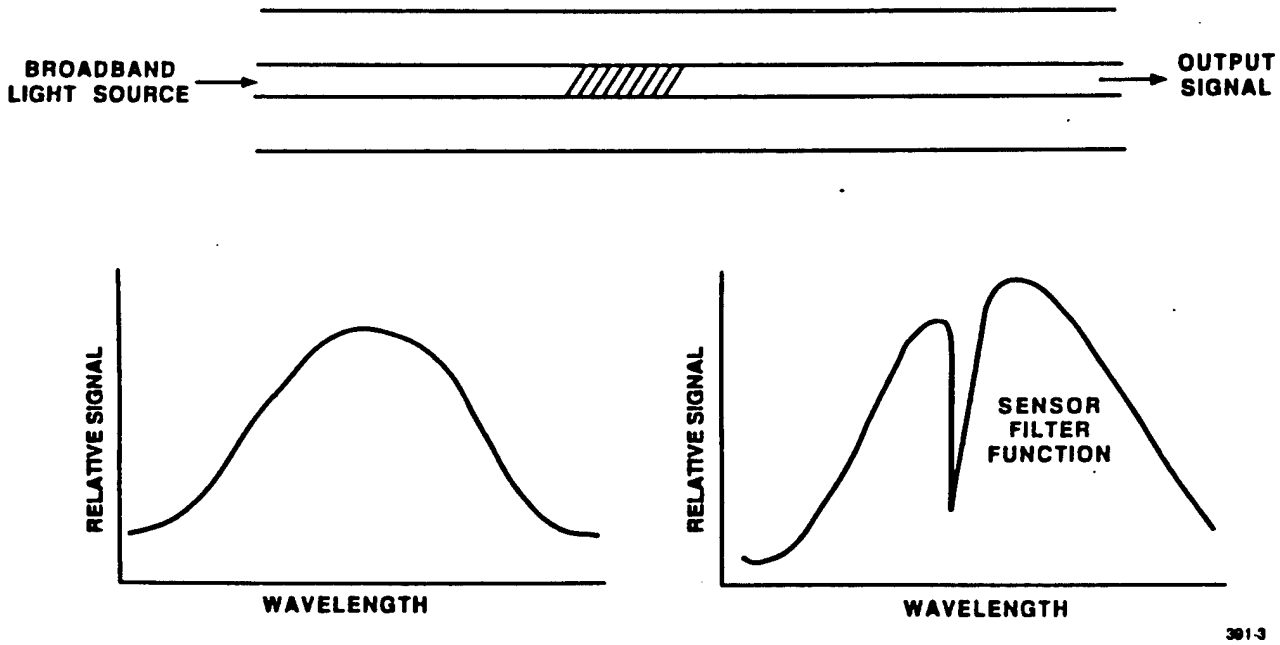

Figure 2. Optical filter function generated by grating

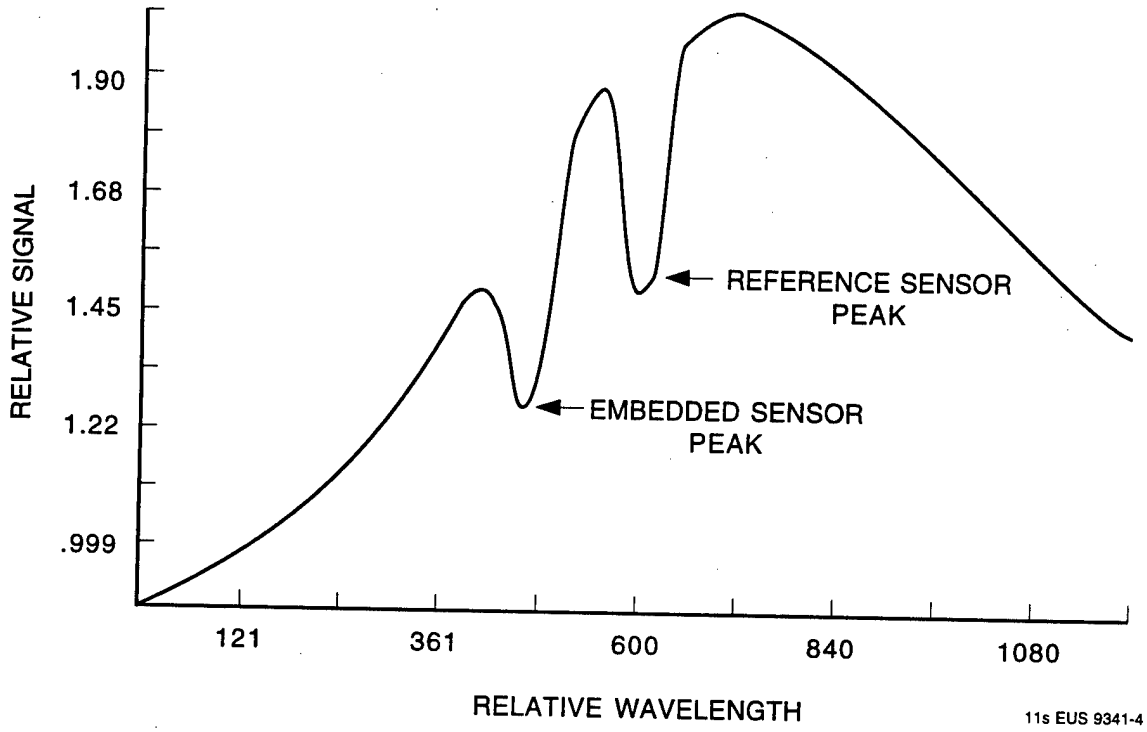

Figure 3. Sample of spectral measurement taken during testing, showing peak for reference sensor and embedded sensor

These devices have been fabricated in optical fibers provided by a variety of vendors, making it feasible to readily supply the Phase I and Phase II programs with unique optical fiber sensors for detecting strain gradient development as a result of residual stresses and post-cure stresses resulting machining and finishing operations.

However, the optical fiber devices must be installed properly to yield the strain measurements. We believe that the primary insertion method of the optical fiber sensors is the translaminar insertion method developed by Foster-Miller.

1.2 Program Summary

The Phase I program showed that through-thickness residual strain in composite parts, due to thermal effects caused by the cure cycle or post-cure machining, could be measured using embedded Bragg grating sensors. Foster-Miller developed novel tooling designs and manufacturing methods to fabricate various composite structures with embedded Bragg gratings.

Average strains along the length of the sensor were measured. Tensile and compressive strain changes were measured during the cutting and drilling experiments. Residual strain could be measured from a distance essentially equal to one laminate thickness, 0.250 in. in this case, away from the embedded sensor.

Residual strain due to thermal effects in the cure cycle was measured in a curved beam. The measured tensile strain of 1234 μin./in. correlated well with the theoretical value of 1208 μin./in. calculated through finite element analysis.

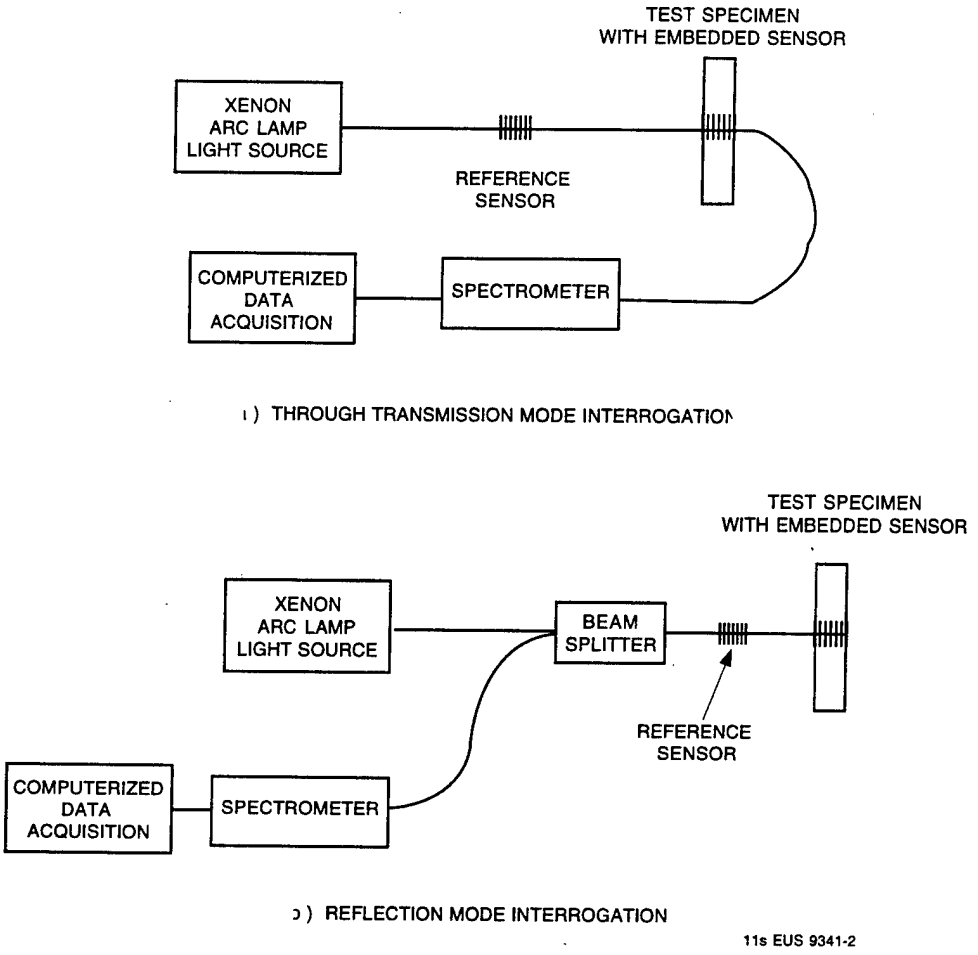

Figure 4. Technique for through transmission and reflection interrogation

1.3 Advantages of the Foster-Miller Approach

Virtually every composite fabrication process inherently results in the presence of residual strains in the component produced. The Foster-Miller approach of embedding fiber optic Bragg grating sensors through the thickness of advanced composite structures allows these strains to be measured directly. Direct measurement of through thickness strain allows for a better understanding of the strain state in the component. These data can be used as tools for quantifying the amount of inherent stresses within the composite structure. This information can be used to validate design and analysis models and could lead to use of higher design allowables.

The Foster-Miller approach offers a number of advantages over currently used strain measurement techniques, such as:

- The sensor can be embedded in either in-plane or through-thickness laminate direction.
- No other known technique can measure translaminar strains directly.
- The insertion technique involves little or no in-plane damage to the composite properties.

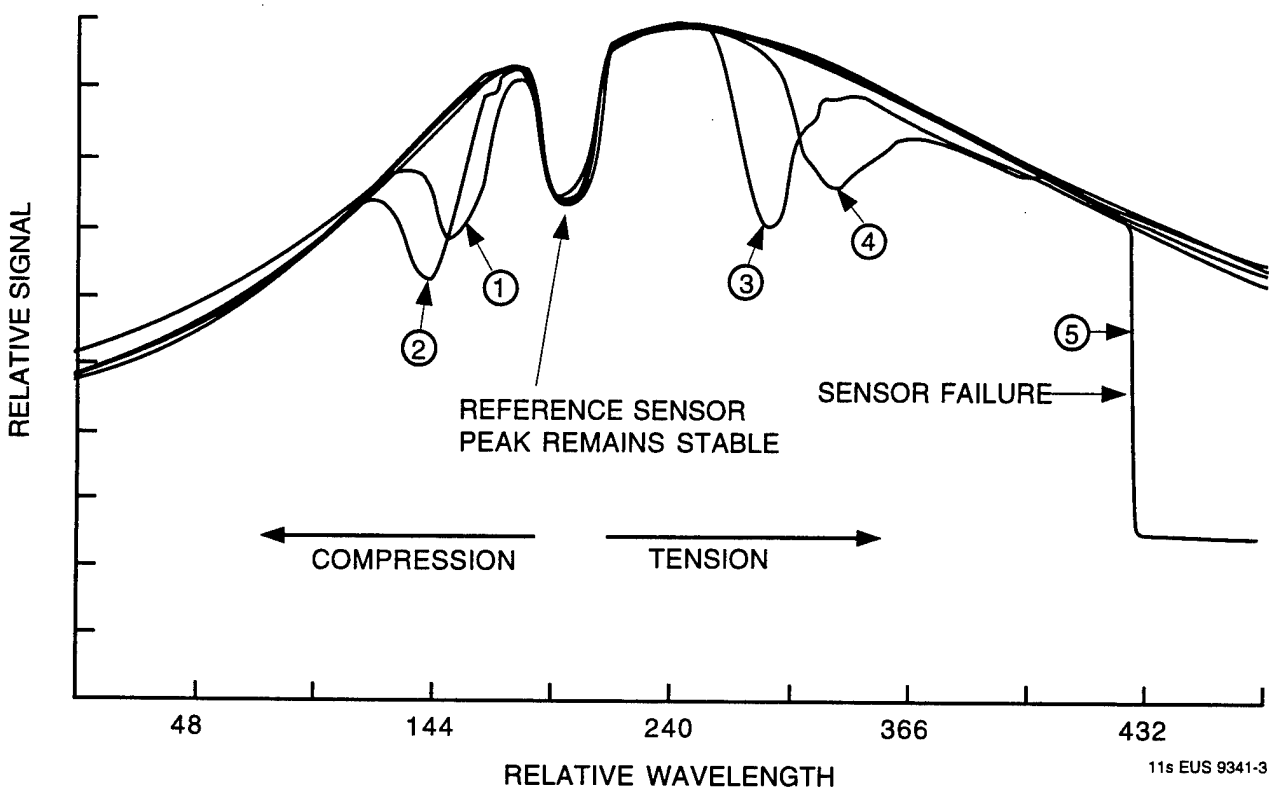

Figure 5. The shift in the filter peak correspond to strain in the embedded sensor

- The sensor can be located exactly where strain measurement is required.
- Dynamic strain measurements can be recorded in real time.
- The technology has the potential for use in a health monitoring system.

During Phase II, these advantages will be exploited to measure residual strain encountered in fulll-scale Navy aircraft composite structures.

2. PHASE I OBJECTIVES

The main objective of this SBIR program was to analytically and experimentally demonstrate the basis for a novel translaminar embedded fiber optic sensor system to directly measure residual strain through the thickness of a high strain Navy aircraft composite part. This objective was essentially met in Phase I by manufacturing advanced composite parts with several embedded Bragg grating sensors used to monitor through thickness residual strain. Strain caused by thermal effects imparted during the cure cycle and strain caused by post-cure cycle machining processes were measured.

Specific technical objectives for the Phase I program included:

- The definition of a "humpback" shaped curved beam representative F18 aircraft component where the ability to measure residual strain could be of significant value to design and production.
- Demonstration that the Foster-Miller ultrasonic fiber-insertion device and novel tooling concept can be used to successfully fabricate components with multiple fiber optic sensors embedded in the translaminar direction.
- Demonstration that the Bragg grating sensor is capable of measuring residual strains resulting from different cure cycles.
- Demonstration that the process can be adapted for use in parts with differing geometries.
- Demonstration that residual strains caused by post-cure machining processes, such as sectioning and drilling, can be measured.

3. PHASE I RESEARCH AND RESULTS

The Phase I research was separated into three interrelated tasks. In this section, the effort conducted on each task to meet the objectives identified in Section 2 is discussed.

3.1 Task 1 - Residual Strain Measurement in a Flat Plate Component

In this task, embedded Bragg grating sensors were used to monitor residual strains caused by post-cure machining processes, such as sectioning and drilling. All the composite components were manufactured at Foster-Miller. United Technologies Research Center (UTRC), our subcontractor, was responsible for the manufacture of all of the Bragg sensors. The machining operations and acquisition of the sensor output were completed at UTRC by both Foster-Miller and UTRC personnel.

All the Bragg grating sensors were manufactured by UTRC to Foster-Miller specifications. The sensors are "written" in the germanium doped core of a silica glass fiber. Each grating was 0.2 in. long with the wavelength written at 1280 nm. A fiber optic pigtail, 3 ft in length, extended from each side of the grating. The sensor was coated with polyimide to protect it from moisture and provide support to deter fracture. Each sensor was treated with an MEK solvent wipe and oven drying step, 220°F for 1 hr, to enhance the sensor to resin matrix bond. The MEK treatment was developed by Foster-Miller on a previously completed SBIR program.

Three composites were manufactured for the testing. One composite was required for the strain measurement during each type of machining, cutting and drilling, while the third was used as a practice component. Each composite had three sensors embedded through the thickness. Figure 6 shows the locations of the embedded sensors. Two of the three sensors were positioned along the same axis while the third was purposely placed off axis in order to evaluate the measured strains as a function sensor position. Three sensors within the composite yielded sufficient means for several strain readings to be taken during the machining of each component.

3.1.1 Flat Plate Panel Manufacture

Three flat plate composite parts were manufactured for this task. Each part was manufactured from AS4/3501-6 uniaxial tape prepreg. AS4/3501-6 is a representative prepreg system used by Navy airframers. The composite size was 4 in. by 8 in. by 0.250 in. Each part had a balanced, 48 ply quasi-isotropic layup, with the 0 deg plies being oriented along the 8 in. direction. Each composite consisted of four 12-ply sublaminates which were laid up and vacuum debulked separately. Each group of four sublaminates was assembled to make a full laminate which was vacuum debulked under a heat lamp for at least 30 min. This "warm" debulk was necessary to compress the laminate thickness to a level close to that of the expected final cure thickness. This step helps to ensure that the sensor remains perpendicular to the laminate surface during processing. The debulked thickness for these parts was about 0.305 in.

The mold components for the flat plate parts were based on a design previously developed by Foster-Miller for a related SBIR program. The mold was designed so that up to three Bragg

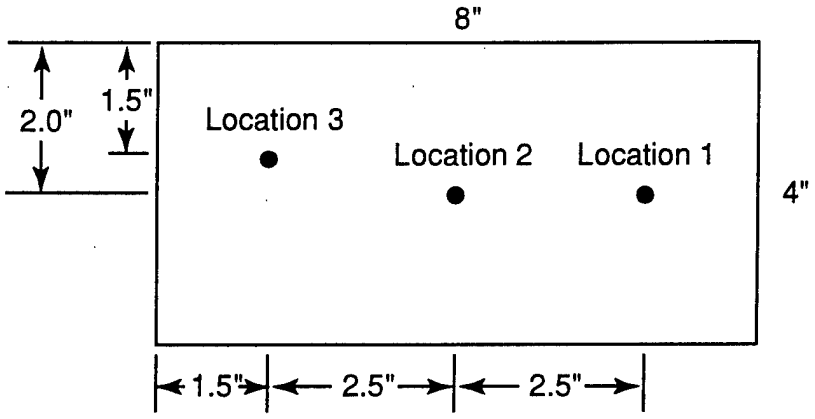

320-NAV-95046-2

Figure 6. Sensor positions in the flat plate composites

grating sensors could be embedded into each composite. One of the three sensor locations was purposely placed off-axis to evaluate residual cure cycle stress as a function of position. A cross-section of the mold is shown in Figure 7. The overall size of the mold was 4 in. by 12 in. The mold components were made out of solid graphite so as to be easily machined and disposable. Salt plugs 1 in. in diameter by 0.250 in. thick were manufactured to be used as

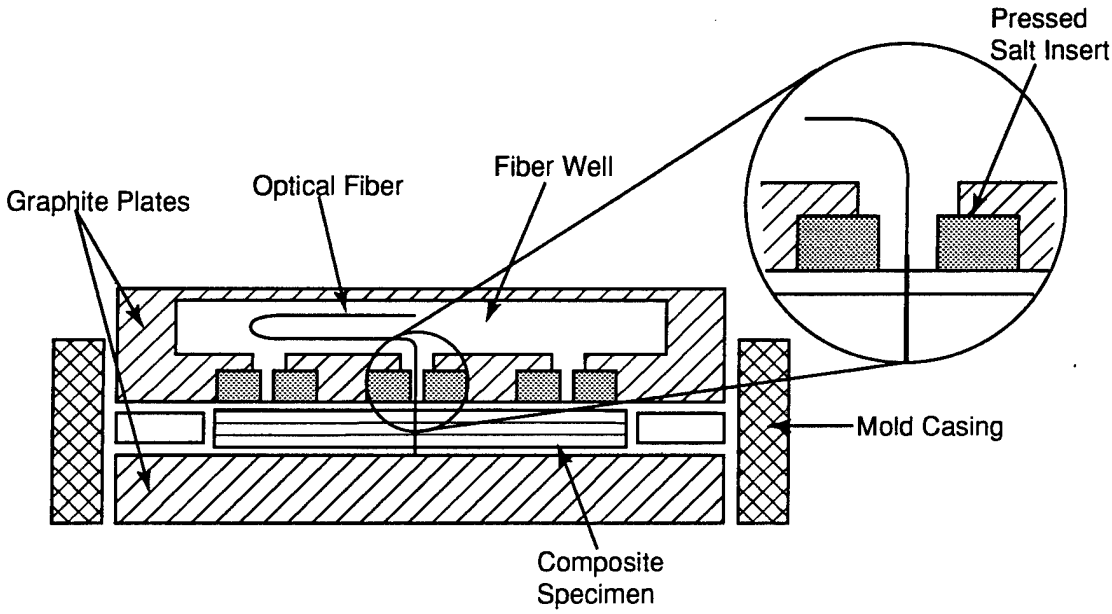

320-NAV-95046-3

Figure 7. Cross-section of the flat plate mold

support and release mechanisms for the fiber optic pigtails. The plugs were manufactured using a steel, compression mold coated with a dry-moly lubricant. Six grams of salt, microsized G95 YPS, were pressed under 20 tons of force to manufacture each plug. The salt plugs were press fit into each mold half. An adequate amount of clear, silicone gel was placed into each countersunk hole prior to the press fit. The silicone gel acted as a barrier/filler to restrict potential resin flow between the mold and salt plug. The two mold halves were clamped together and a 40 mil diameter hole was drilled through each of the salt plugs.

Each mold was sealed with a thin coating of sodium silicate solution. The sealed mold components were subsequently release coated with Frekote 44. A mold casing, made from 1/8 in. thick aluminum bar stock, which was designed and fabricated to fit snugly around the graphite mold was also release coated. The casing was deemed necessary so as to keep the mold halves from shifting. Any significant shift was previously found to cause one or both fiber optic ends to be sheared off at the composite/mold interface. Steel bolts were used to connect the mold halves and spacers within the mold casing.

Each part was positioned in the completed mold setup, including the casing, with non-porous and porous Teflon layers at each composite/mold interface. The Teflon layers aided part removal. Three holes were made through each composite using a modified ultrasonic process. Each hole was positioned in the center of the previously drilled holes within the salt plugs. The diameter of the ultrasonically formed holes was about 15 to 20 mils. An MEK wiped Bragg grating sensor was fed through each hole. The Bragg grating length was centered within the composite thickness. Once the sensors had been positioned, each hole in the salt plugs was filled with a room temperature cure silicone gel used to encase the fiber optic. Not only did the silicone act as a barrier to impede resin flow but it also served as a stress relief mechanism for the fiber at the composite surface.

3.1.2 Measurement of Strain Caused by the Embedding Process

A connector was epoxied on one pigtail end of each Bragg sensor. Spectrometer readings were taken at UTRC. A comparison of the embedded spectral reading to that of the unembedded sensor (taken at UTRC at the time of manufacture) shows the amount of strain caused by the embedding process. Figure 8 shows the spectrometer readings of a sensor in its unembedded and embedded state. The change in the wavelength at the peak of the reflection curve, in nanometers, can be directly converted to strain.

Table 1 summarizes the spectrometer readings taken on each sensor prior to and after the embedding process. All of the sensors were embedded after complete debulk of the laminate. The Bragg gratings in the flat plates had a range of residual strain change due to the embedding process of 624 to 936 μin./in. This range was greater than was expected. It was expected that the embedding process would yield zero strain on a flat plate. The change in strain was probably due to the fiber optic not being embedded into a tight fitting hole. An analysis was completed to assess the amount of strain that could be imparted into the sensor due to bending. Figure 9 shows a conceptual drawing of the embedded sensor in an uncured composite. Based on strain=(d/2)/R where R is the radius of curvature and d is the sensor diameter, it was calculated that a strain of up to 3390 μin./in. could be realized if the sensor was fully bent within the composite. Although the measured, embedded sensor strain value was less than 25 percent of the maximum possible calculated strain, extra care will be taken to alleviate any bending of the sensor in subsequent composite parts.

Once the spectral measurements had been taken on all the embedded sensors, each pigtail length was wound into a circle and secured in the fiber well of the mold. Release coated aluminum caul plates were positioned on top of each fiber well to protect the pigtails during autoclave processing. Autoclave processing followed the standard procedure developed by

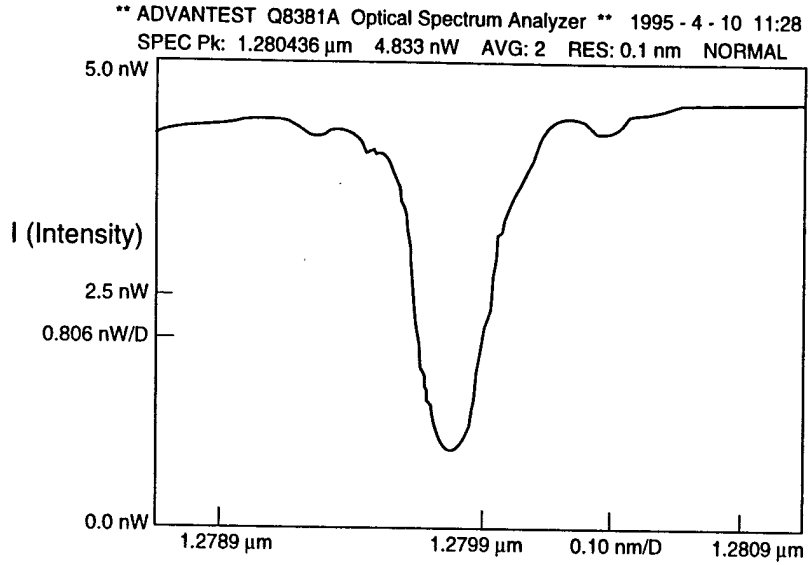

State of Sensor	Wavelength, λ of Peak Reflectivity (nm)	Difference (nm)	Strain (µ)
As Fabricated	1279.802	------	------

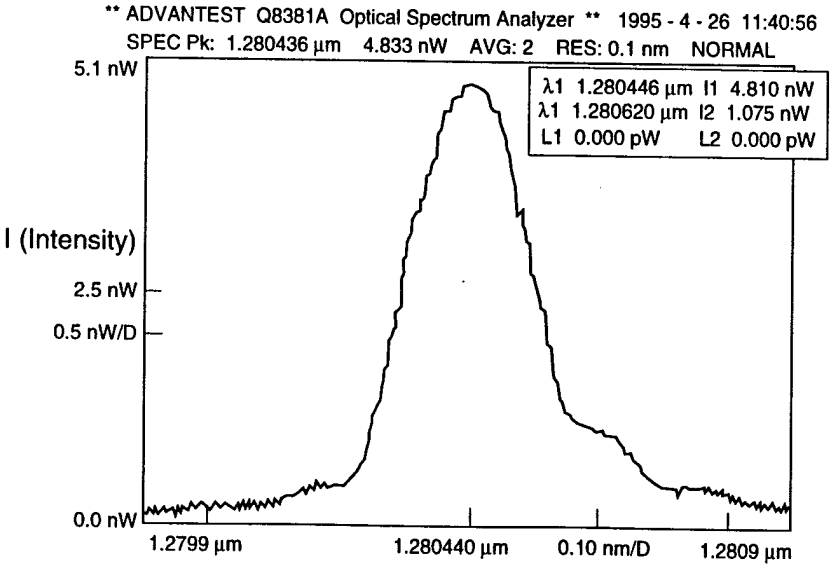

State of Sensor	Wavelength, λ of Peak Reflectivity (nm)	Difference (nm)	Strain (µ)
After Embedding	1280.436	0.634	634

318-NAV-95046-13

Figure 8. Strain calculation via wavelength shift

Table 1. Residual strain due to the embedding process

	FP3 S1*	FP3 S2	FP3 S3	FP1 S1	FP1 S2	FP1 S3	FP2 S3
Peak spectrometer reading							
Before embedding (nm)	1279.812	1279.82	1279.832	1280.352	1280.34	1280.264	1279.812
After embedding (nm)	1280.67	1280.746	1280.768	1281.152	1281.076	1281.104	1280.436
Residual strain due to embedding (μin./in.)	858	926	936	800	736	840	624

*Note: FP 3S1 refers to flat plate No. 3 sensor No. 1.

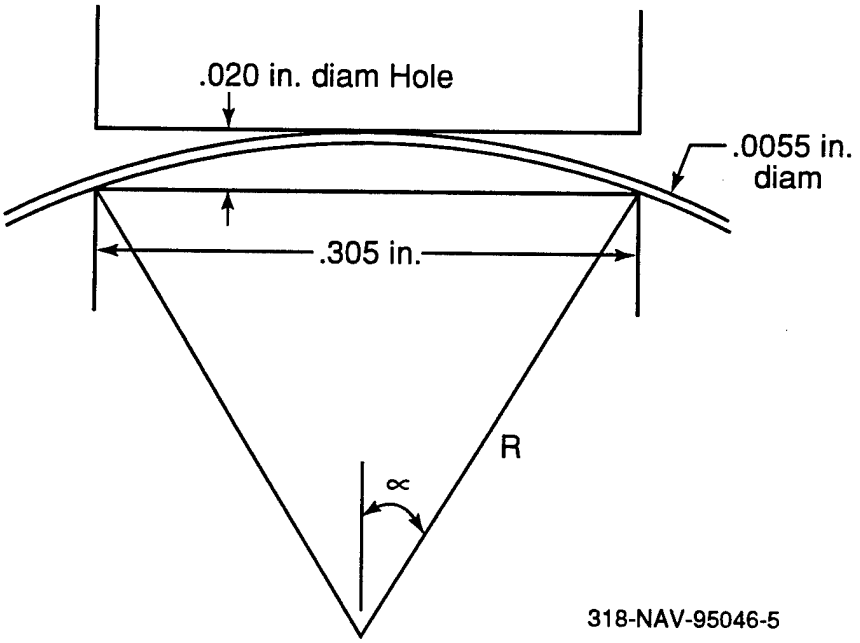

Figure 9. Potential bending strain on an embedded sensor

* Foster-Miller. Each of the three components was cured using a modified 350°F cure cycle.
* Pressure (100 psi) was applied after the part temperature reached 200°F. At this temperature
* the viscosity of the matrix resin is at a minimum so that if the Bragg grating shifts due to
* compaction of the composite, it can move without fracturing. Figure 10 shows the cure cycle.

After the cure cycle, each mold setup was removed from the vacuum bag. The salt plugs were dissolved away with a warm water stream. Spectral measurements were taken on each of

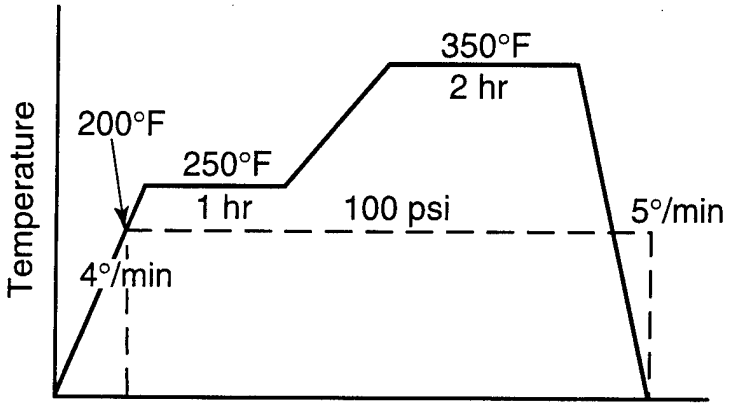

Figure 10. Modified autoclave cure cycle

the sensors at UTRC. These readings served as the "zero" point for all the subsequent spectrometer readings acquired during the machining experiments.

3.1.3 Measurement of Residual Strain due to Machining Operations

All three flat plate composite parts were machined at UTRC. Flat plates No. 1 and No. 2 served as the specimens for the sawcut experiment while flat plate No. 3 was used for the drilling experiment. Spectral readings were acquired using an Advantest Optical Spectrum Analyzer equipped with a Milles Griot Diode Laser Driver and a Light Control Instruments Temperature Controller. All spectrometer readings were taken once the machined composite had cooled to room temperature. Real time data acquisition was accomplished by adding a Dolch portable computer into the setup. A standard cut-off saw with a diamond tipped blade was used for the machining of flat plates No. 1 and No. 2. The saw blade width was 0.04 in. and the blade diameter was approximately 7 in. A standard drill press was used along with standard drill bits for the drilling experiments on panel No. 3.

Residual Stress due to Sectioning

Several longitudinal (i.e. along the 8 in. direction of the plate) and lateral (i.e. along the 4 in. direction) cuts were made at various distances from the sensor location to evaluate the magnitude of residual strain. Spectrometer readings were acquired before and after each cut. Flat plates No. 1 and No. 2 were used for this experiment. Table 2 summarizes the residual strain results.

A longitudinal cut was made at a location 0.250 in. and then 0.125 in. from the position of sensor No. 2 in flat plate component No. 1. Figure 11 shows the spectrometer readings acquired. The residual compressive strain due to the first cut was 240 μin./in. By subsequently machining a free edge closer to the sensor (0.125 in.) the cumulative residual compressive strain increased to 470 μin./in.

A single longitudinal cut was made 0.250 in. away from sensor No. 3 in flat plate No. 1. Figure 12 shows a slight shift in the peak corresponding to a compressive strain of only 30 μin. This value is lower than that measured by sensor No. 2 under the same conditions. Upon inspection it was found that the sensor was not fully embedded into the laminate. This resulted in a "lower" strain reading due to the averaging effects of the grating.

Table 2. Summary of residual strain due to sectioning

	Spectrometer Readings				
	Start (nm)	Finish (nm)	Difference (nm)	Strain (μ in./in.)	Cumulative Strain (μ in./in.)
FP1, Sensor 1					
Before cutting	-	1280.7	-	-	-
1/4 in. cut lateral	1280.7	1280.5	-0.2	-200	-200
1/8 in. cut lateral	1280.5	1280.45	-0.05	-50	-250
FP1, Sensor 2					
Before cutting	-	1282.26	-	-	-
1/4 in. cut long.	1282.26	1282.02	-0.24	-240	-240
1/8 in. cut long.	1282.02	1281.79	-0.23	-230	-470
FP1, Sensor 3[1]					
Before cutting	-	1280.23	-	-	-
1/4 in. cut	1280.23	1280.2	-0.03	-30	-30
1/4 in. cut lateral 90 deg	1280.2	1280.17	-0.03	-30	-60
1/8 in. cut lateral (same as above)	1280.17	1280.22	0.05	50	-10
FP2, Sensor 3					
Before cutting	-	1271.86	-	-	-
1/4 in. cut lateral	1271.86	1271.84	-0.02	-20	-20
1/8 in. cut lateral	1271.84	1271.71	-0.13	-130	-150
1/16 in. cut lateral	1271.71	1271.8	0.09	90	-60

[1]Not fully embedded.

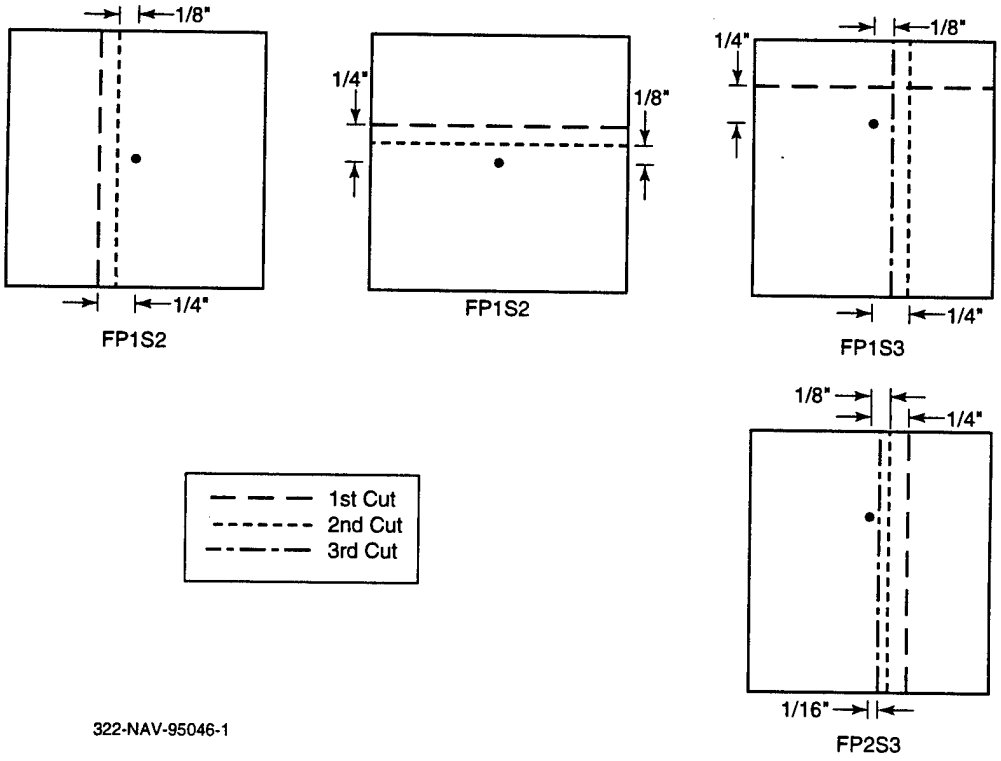

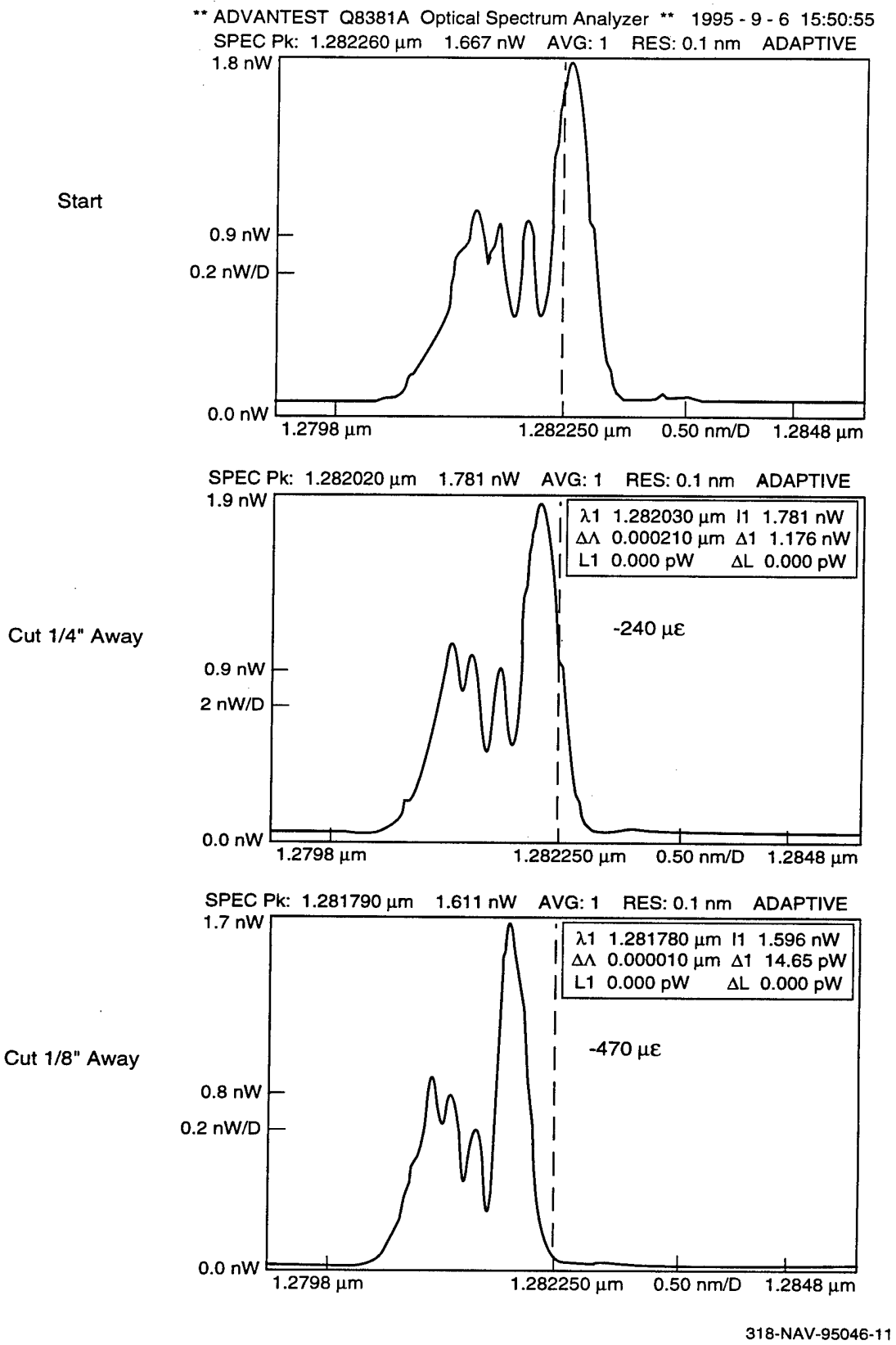

Figure 11. Peak shift in sensor No. 2, flat plate No. 1

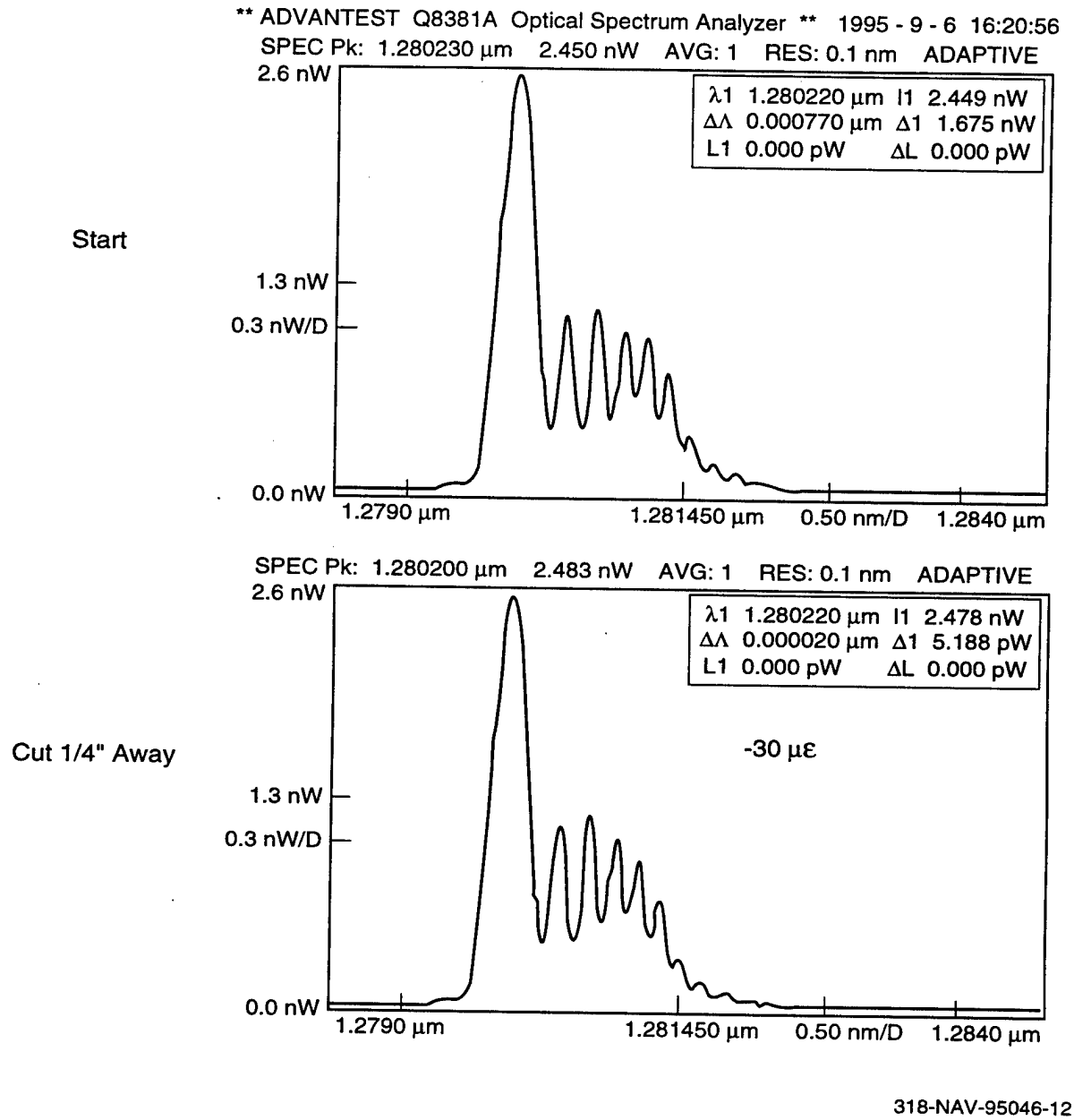

Figure 12. Peak shift in sensor No. 3, flat plate No. 1

Three lateral cuts were made at various distances from sensor No. 3 in flat plate No. 2. Sensors No. 1 and No. 2 were damaged prior to testing. Figure 13 shows the spectrometer readings acquired. The cumulative residual compressive strain increased from 20 to 150 μin./in. when the distance of the free edge to the sensor was decreased from 0.250 to 0.125 in. Upon a further decrease in distance to 0.0625 in., a decrease in the cumulative strain, to 50 μin./in., was seen. This represents a positive (tensile) change in strain of 100 μin./in.

There are three phenomena that could contribute to the residual strain measurements recorded during the sawcutting experiment. The first is strain due to the temperature change in the composite caused by the friction of the cutting blade against the composite surface. This does not represent a permanent strain and any effects would disappear as the composite cooled to room temperature (which represents the point at which the spectrometer readings were taken).

The second potential cause is tearing of the composite by the cutting blades. Residual strain would occur if microcracks were formed. If the microcracks led to delaminations, the strains would be positive because the sensor would restrain the crack opening tendency. This is what caused the positive change in strain for sensor No. 3 embedded in flat plate No. 2 (described above). As the cut was made closer to the sensor, the delaminations caused by the cut moved to the sensor position causing the positive (tensile) strain change. However, this would be a very local effect and would not generate significant strains unless visible delaminations were present.

The final potential cause of residual strain is interlaminar stress which forms at the free edge to balance the change in the stress state caused by differences in Poisson's ratio through the thickness of the composite. The magnitude of the strains created at the free edge are dependent upon the layup and the orientation of the plies. Figure 14 shows the distribution of interlaminar normal stress on a typical laminate midplane. These strains are also very local. A separate analysis of the free-edge stress on the specific flat plate used needs to be conducted to verify this source of strain.

Figure 15 shows the residual strain as a function of the distance from the position of the cut to the sensor location. No residual strain values were recorded when the cuts were further than 0.250 in. away from the sensor. As the distance of the free edge to the sensor decreased from 0.250 to 0.125 in. the average (of three individual cuts) residual compressive strain increased from 150 to 290 μin./in. Although there is a small amount of scatter in the individual readings, in all three cases the compressive strain at a cut distance of 0.125 was greater than the corresponding strain value at 0.250 in. cut distance. On the one occasion where an even closer cut was possible, 0.065 in. away from the sensor, the compressive strain decreased to a value of 60 μin./in.

A small section of sensor No. 3 in flat plate No. 1 was not fully embedded in the composite. During the sawcutting experiment the spectral peak for this section of sensor was tracked in real time (see Figure 16). Two large changes in the peak value occurred. These changes in the peak were due primarily to the change in temperature associated with the cutting experiment. As the composite absorbed heat during the sawcut operation, the sensor (outside the composite) would strain based on its CTE of 5×10^{-7} mm/mm °C. Based on this CTE value a change in wavelength of 1×10^{-2} nm would yield a 1°C temperature change. Figure 17 shows the calculated temperature change based on the shift in the peak value.

The first major change occurred in the 370 to 600 sec time range. At a time of 370 sec the leading edge of the sawblade was at a position, during a cut at 0.250 in. away from the sensor, where the residual heat began to strain the unembedded section of the sensor. At 410 sec, the

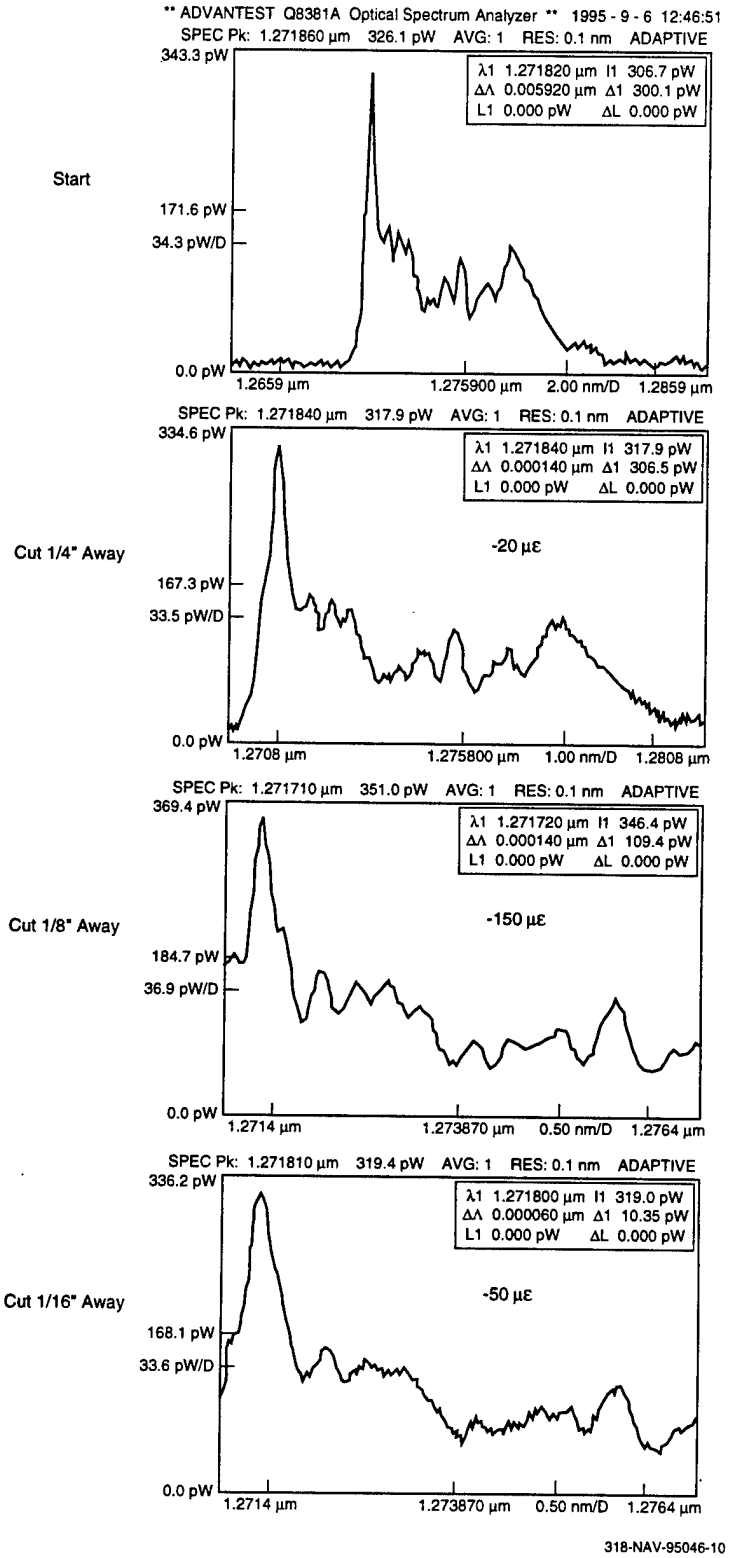

Figure 13. Peak shift in sensor No. 3, flat plate No. 2

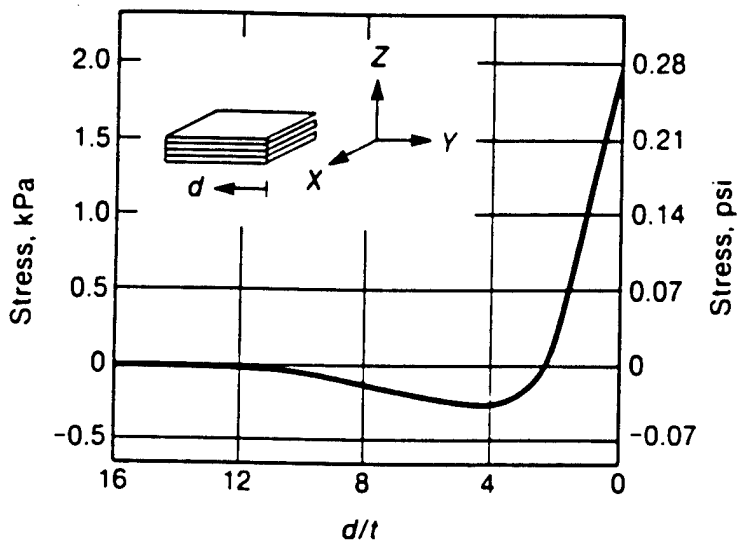

Figure 14. Distribution of interlaminar stresses

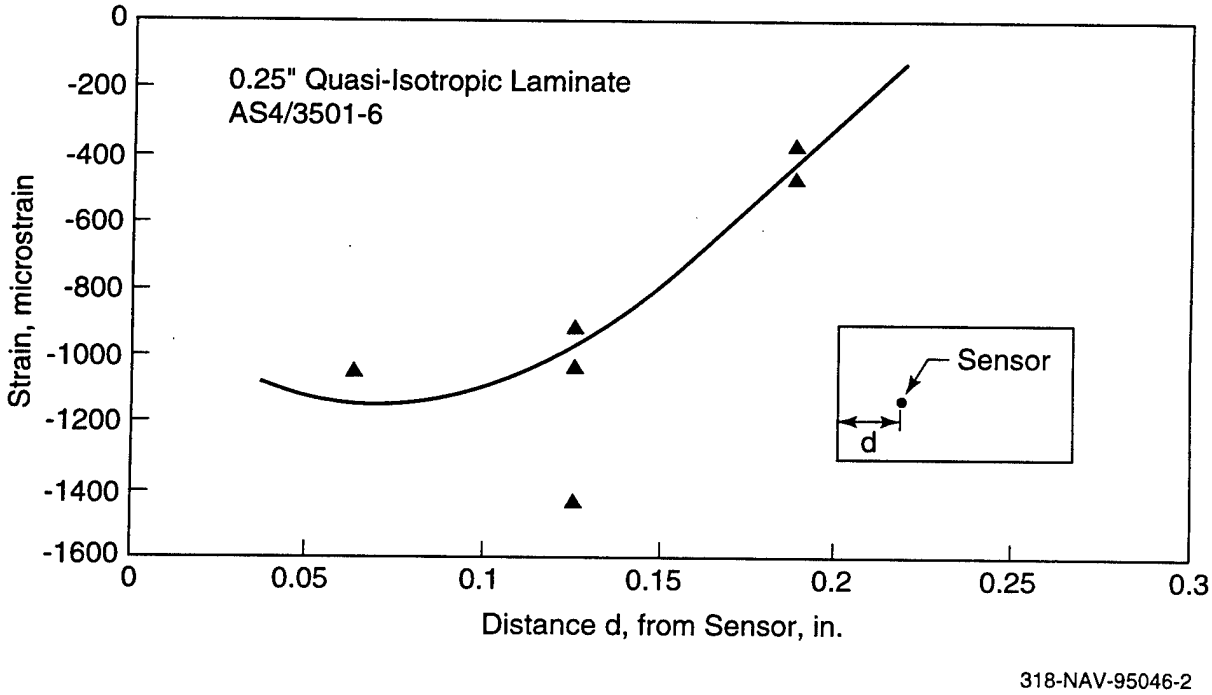

Figure 15. Through-thickness residual strain as a function of distance from machined edge

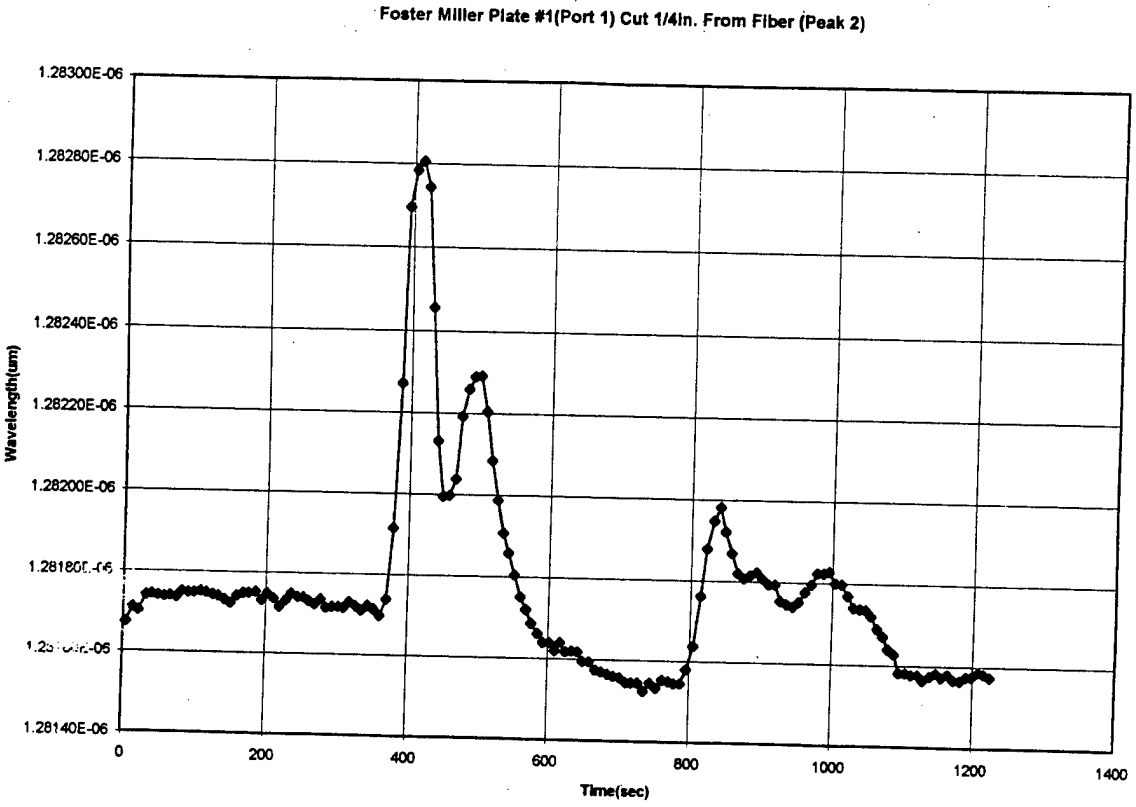

Figure 16. Real time data for peak shift due to residual heat

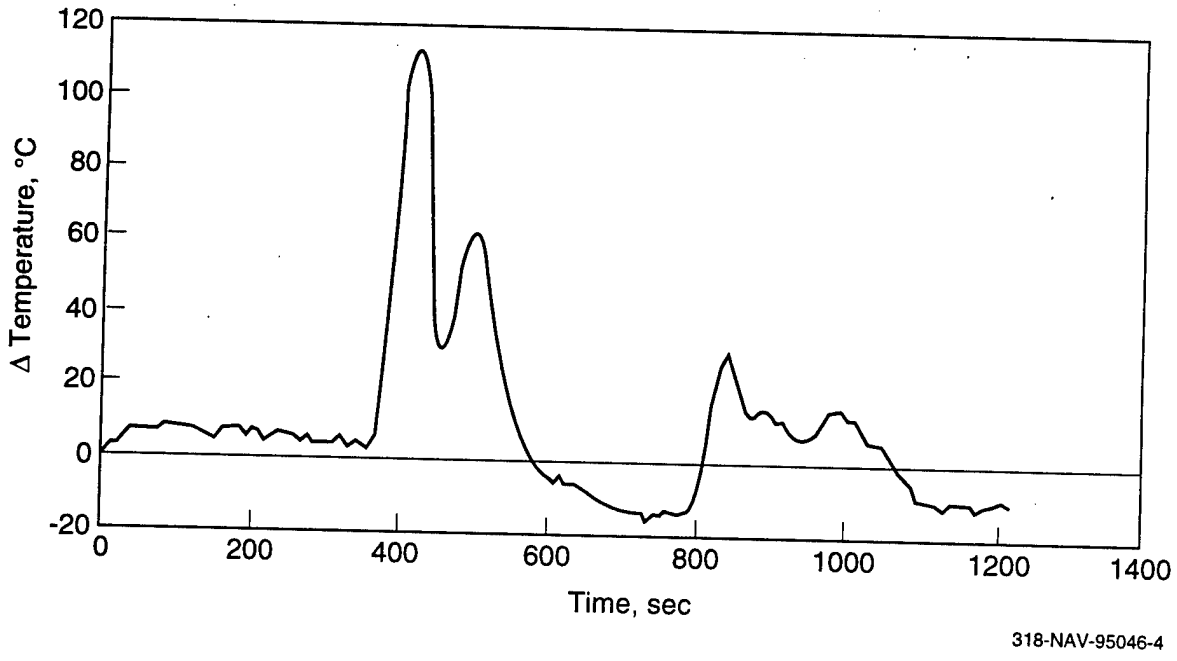

Figure 17. Calculated temperature change based on peak shifts

leading edge was parallel to the sensor and the maximum temperature change occurred. As the leading edge moved away from its parallel position the residual heat started to decrease until the trailing edge of the sawblade moved into a position parallel to the sensor. The trailing edge yielded a smaller peak change whose maximum occurred at 510 sec. As the sawblade was retracted a small temperature change was seen in the 800 to 1100 sec time range.

In Phase II, thermal imaging techniques and/or thermocouples should be used to confirm the larger than expected temperature increase measured by the Bragg grating.

Measurement of Residual Stress caused by Drilling

Flat plate No. 3 was used for the drilling experiment. Two different diameter bits, 0.125 and 0.250 in., were used to drill sets of holes in close proximity to each of the Bragg grating sensors. Several holes were drilled around each embedded sensor. Table 3 summarizes the measured strain and shows a schematic of the location of each drilled hole. The distance from the sensor is based on the distance from the center of the drill bit to the sensor location.

Four holes were drilled around sensor No. 1 at a distance of 0.250 in. Figure 18 shows the peak shift in the spectrometer readings taken after the completion of each drilling step. After each successively drilled hole, the spectral peak shifted to the left indicating a compressive strain on the composite. As expected, the cumulative strain increased after each hole had been drilled. The measured strains were negative because the crack fronts, caused by the drilled holes at 0.250 in. away, did not propagate to the sensor location.

Three 0.250 in. diameter holes were drilled around sensor No. 2. Each hole was drilled at a different (i.e. closer) distance. Figure 19 shows the spectrometer readings. The tall peak to the right represents a portion of the sensor that extended out of the composite while the smaller peak to the left represented the section of the embedded sensor. By tracking the peak to the left it was found that the original hole, at a 0.250 in. distance, produced a strain of 1192 μin./in. Each of the two subsequent holes was drilled at a position closer to the sensor. In both cases the peak shifted back to the right indicating a positive strain change which decreased the amount of cumulative compressive strain. This was anticipated due to the fact that when the free edge is machined close enough to the sensor, any delaminations caused by the machining propagate past the sensor causing the grating to be put in tension.

Two different diameter (0.125 and 0.250 in.) holes were drilled around sensor No. 3 at a location 0.250 in. away from the sensor. Figure 20 shows the correlation between the strains measured by sensors No. 1 and No. 3. Approximately 350 μin./in. of compressive strain was measured for each 0.125 in. diameter hole drilled 0.250 in. away from the sensor. For each 0.250 in. hole, drilled 0.250 in. away, the measured compressive strain was about 1000 μin./in.

A graph of distance versus measured strain for the drilling experiment is shown in Figure 21. The distance for this figure was defined as the distance from the free edge of the hole to the sensor location. This figure also shows the data from the cutting experiment. As the distance of the free edge to the sensor decreases from 0.1875 to 0.125 in. the residual compressive strain increases from 380 to 1020 μin./in. On the one occasion where a hole was drilled closer to the sensor, free edge at 0.0625 in., the residual compressive strain was 1100 μin./in.

3.2 Task 2 - Residual Strain Measurement in an Angled Beam

In this task, embedded Bragg grating sensors were used to monitor residual strains due to thermal effects induced during the cure cycle. An angled beam was chosen as the component

Table 3. Summary of residual strain due to drilling

Flat Plate No.	Sensor No.	Hole Size (in.)	Distance from Sensor (in.)	Spectrometer Reading (nm) Before	Spectrometer Reading (nm) After	Difference (nm)	Change in Strain (μin./in.)	Cumulative Strain (μin./in.)
3	1		Before drilling	-	1280.724	-	-	-
-		1/8	0.25 in. away	1280.724	1280.344	-0.38	-380	-380
		0.25	0.25 in. away	1280.344	1279.804	-0.54	-540	-920
			Same, 90 deg from 1st	1279.804	1279.604	-0.2	-200	-1120
			Same, 180 deg from 1st	1279.604	1278.704	-0.9	-900	-2020
3	2		Before drilling	-	1280.782	-	-	-
		0.25	0.25 in. away	1280.782	1279.59	-1.192	-1192	-1192
			3/16 in. away	1279.59	1279.98	0.39	390	-802
			5/32 in. away	1279.98	1280.16	0.18	180	-622
3	3		Before drilling	-	1279.764	-	-	-
		1/8	0.25 in. away	1279.764	1279.384	-0.38	-380	-380
		0.25	0.25 in. away, 180 deg	1279.384	1278.724	-0.66	-660	-1040

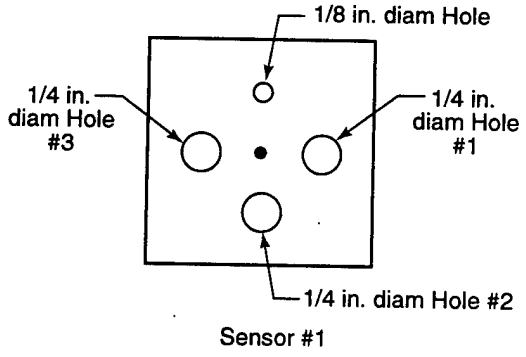

Sensor #1

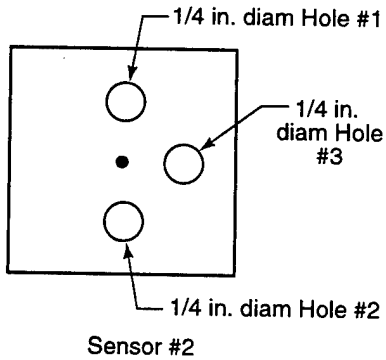

Sensor #2

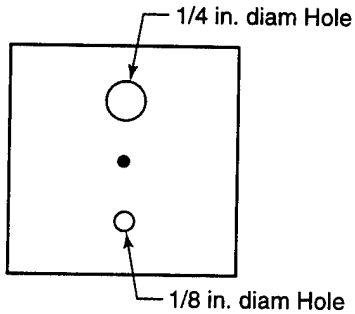

Sensor #3

318-NAV-95046-1

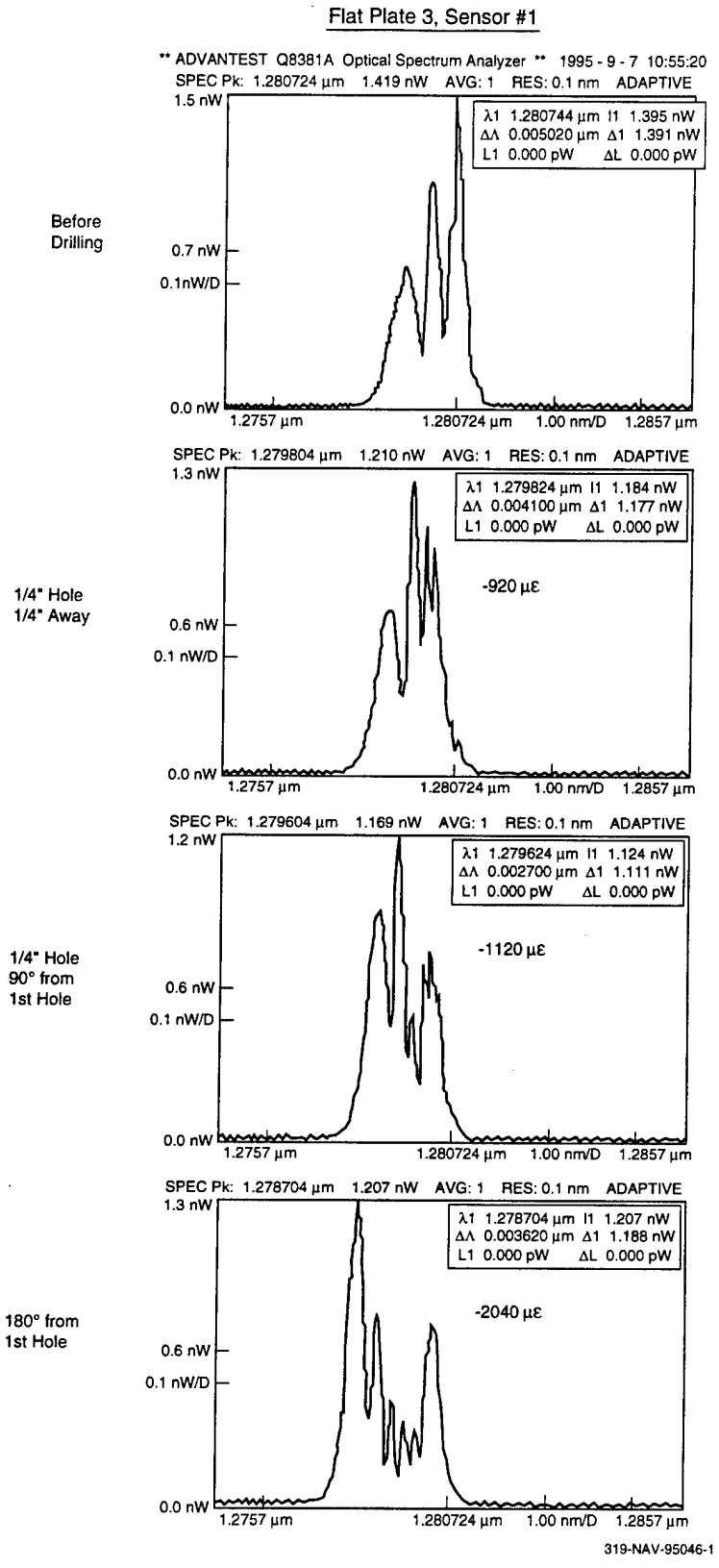

Figure 18. Peak shift in sensor No. 1, flat plate No. 3 during drilling

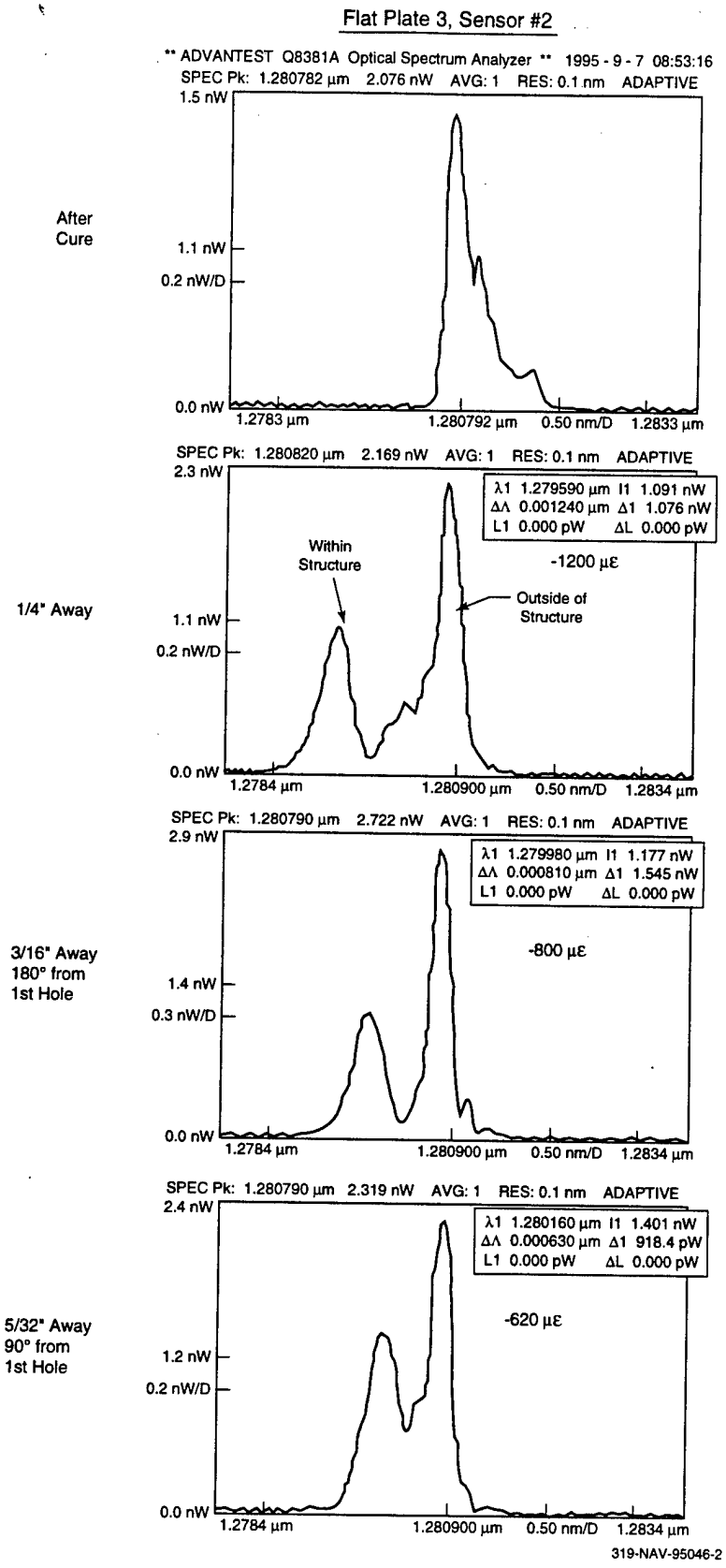

Figure 19. Peak shift in sensor No. 2, flat plate No. 3 during drilling

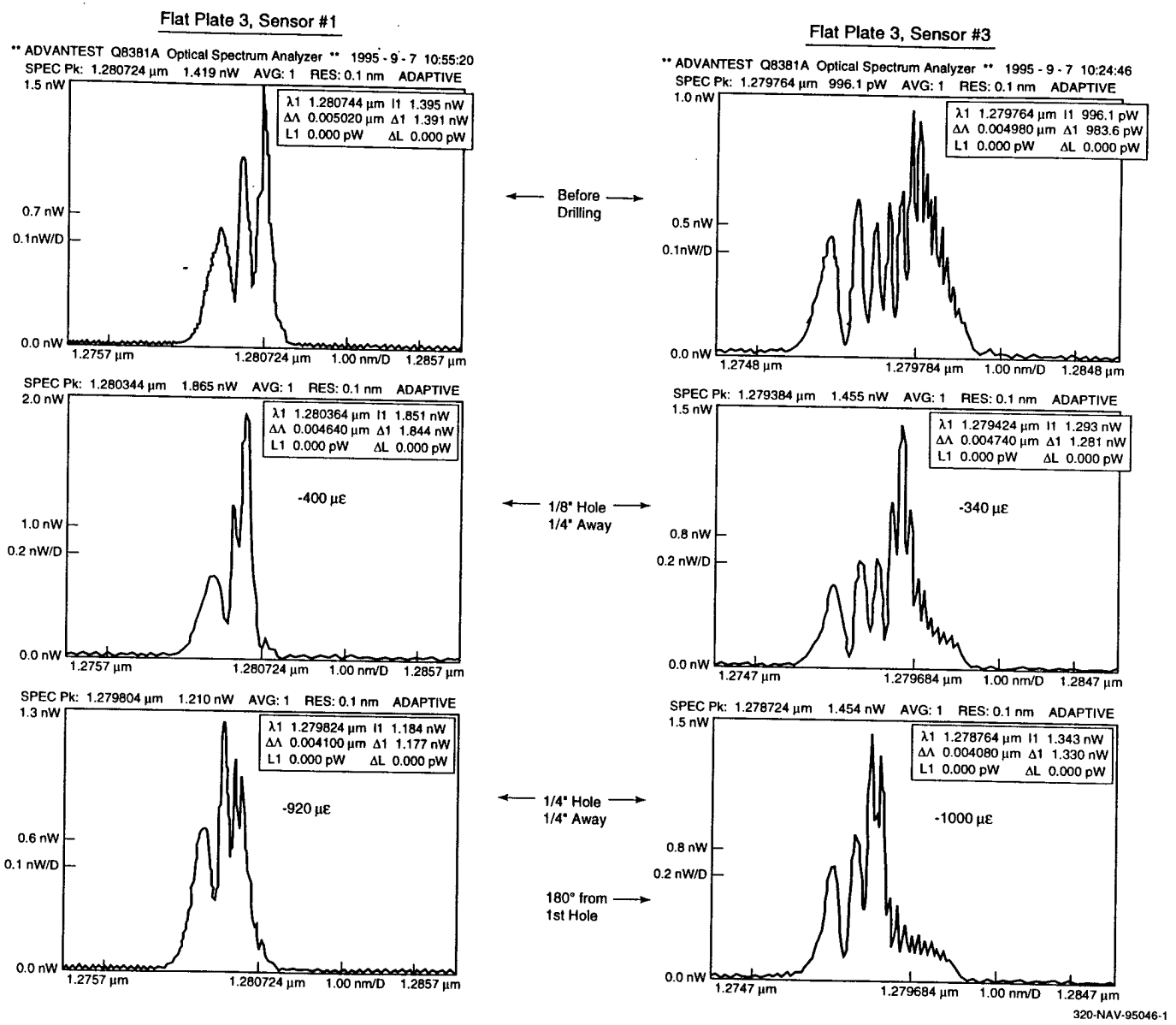

Figure 20. Strain correlation from sensors No. 1 and No. 3

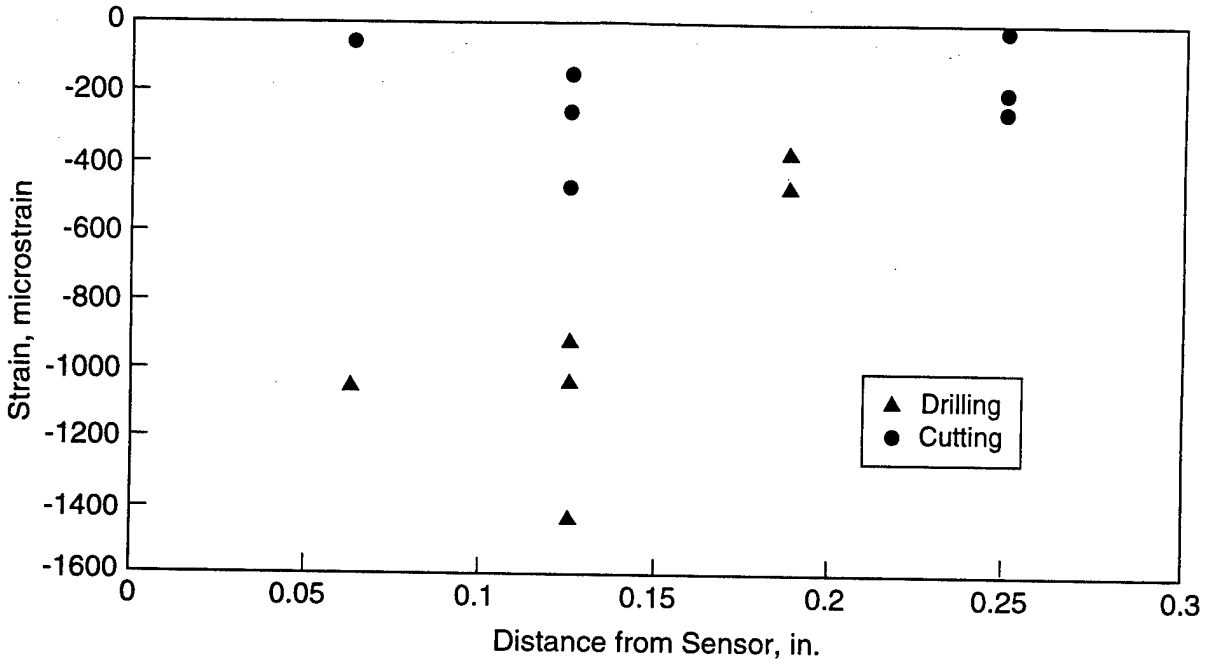

Figure 21. Strain versus free edge distance

on which the residual strain was measured. The angled beam was chosen to represent a high-strain humpback on the F-18. A single fiber optic Bragg grating was embedded in each angled beam. A residual strain of 1234 μin./in. was measured for one component. This measured value correlated well to a finite element analysis on an identical angled beam with a similar layup that predicted a strain of 1208 μin./in.

3.2.1 Manufacture of Angled Beams

The sensors that were designed for this task were exactly the same as those used in Task 1. The only difference is that one of the pigtails was eliminated to allow insertion where access from only one side was possible. "Dead ending" the sensor allowed for a simpler mold design and manufacturing process.

The angled beam component chosen as a representative F-18 "humpback" design is shown in Figure 22. This component is a right angle beam with an inner radius of 0.125 in. A mold was designed for the manufacture of this component based on Foster-Miller's expertise in novel tooling concepts for through thickness embedded fiber optic sensors. Each component was designed to be 4 in. wide. Figure 23 shows a schematic view of a cross section of the mold. Two molds and a mold casing were manufactured from aluminum.

A trial component was manufactured from AS4/3501-6 uniaxial tape prepreg to verify the manufacturing process (detailed in subsection 3.1.1). The part layup was [+45 deg, -45 deg] 12S which yielded a cured part thickness of 0.250 in. A dummy sensor, i.e. fiber optic with no Bragg grating, was embedded through the thickness of an angled beam component in the radius section. The composite part was autoclave cured using the modified 350°F cure cycle (Figure 10). The angled beam was removed from the mold with the dummy sensor intact.

Three angled beam test components were fabricated for measurement of residual stresses due to thermal effects caused by the cure cycle. The first angled beam had a [+45 deg, -45 deg]

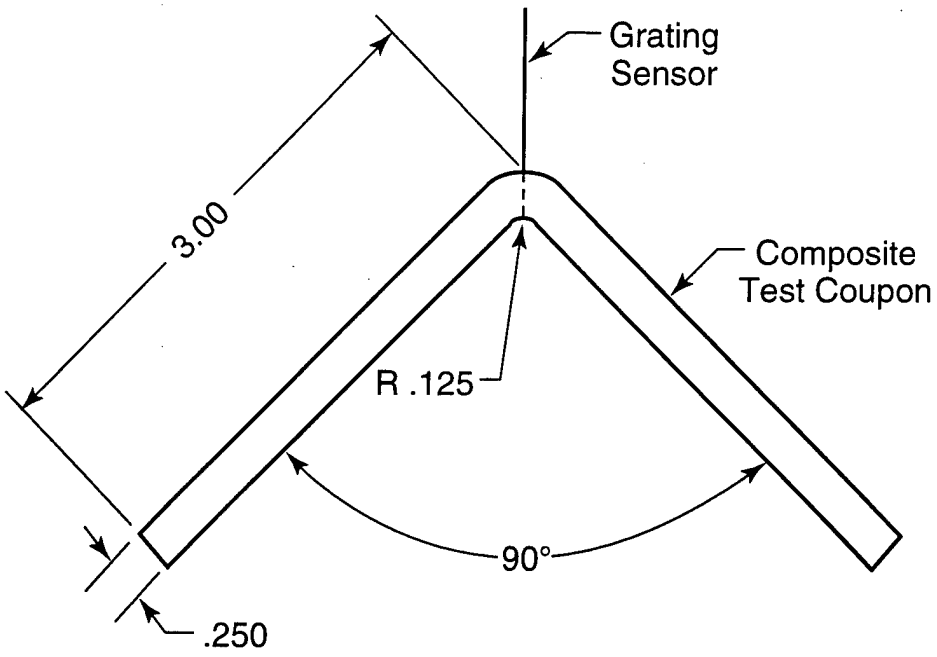

Figure 22. Side view of the angled beam

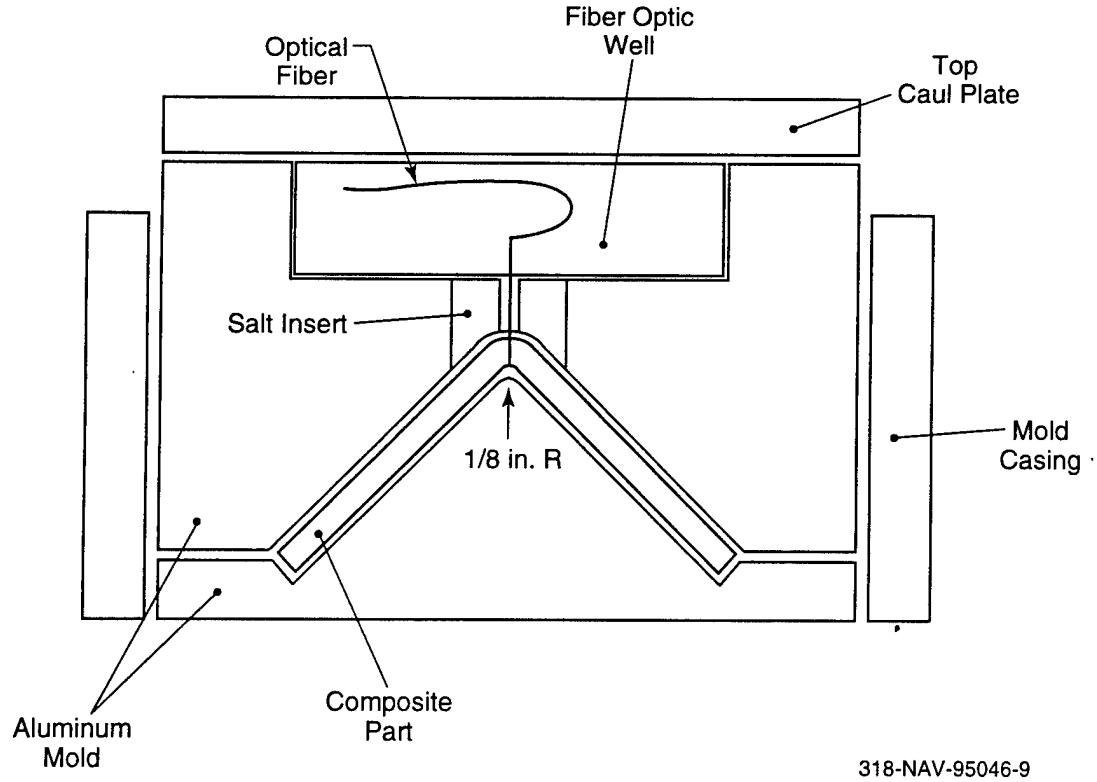

Figure 23. Cross-section of the angled beam mold

12S layup while angled beams No. 2 and No. 3 had a [0 deg, 90 deg] 12S layup. A single dead ended sensor was embedded through the thickness at the radius of each composite using Foster-Miller's modified ultrasonic technique. Angled beams No. 1 and No. 3 were cured using the modified 350°F cure cycle previously shown in Figure 10. Angled beam No. 2 was cured using a different cure cycle, shown in Figure 24. Different layup configurations and cure cycles were used to examine their effects on residual stress.

3.2.2 Residual Strain Measurement

For each of the three angled beams, three individual spectrometer readings were taken for each sensor. The three readings taken were after sensor manufacture, after embeddeding in the uncured composite and after complete cure of the composite. Table 4 summarizes the spectrometer readings and the corresponding strain changes.

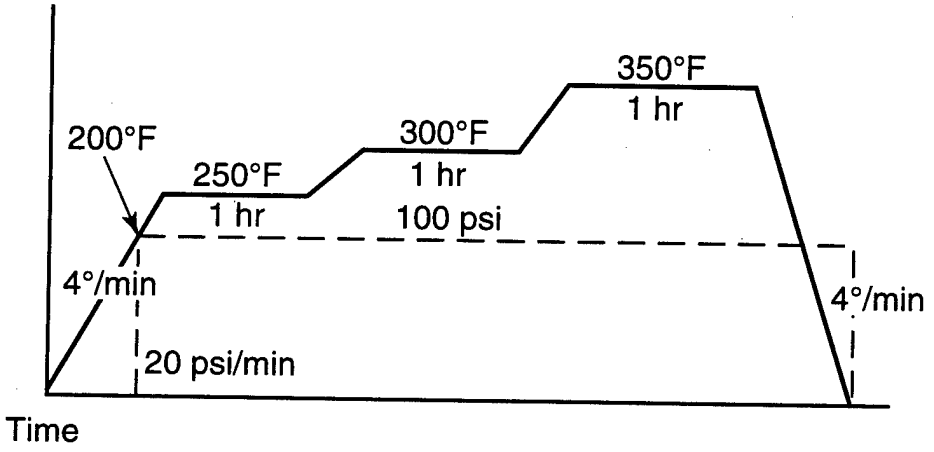

Figure 24. Modified autoclave cure cycle

Table 4. Residual strain results for the angled beams

Angled Beam No.		Spectrometer Readings (nm)			Change in Strain (μin./in.)	Cumulative Strain (μin./in.)
		Before	After	Difference		
1	Before embedding	-	1280.304	-	-	-
	Before cure	1280.304	1279.46	-0.844	-844	-844
	After cure	1279.46	1280.694	1.234	1234	390
2	Before embedding	-	1280.67	-	-	-
	Before cure	1280.67	1280.714	0.044	44	44
	After cure	1280.714	1271.18	-9.534	-9534	-9490
3	Before embedding	-	1280.764	-	-	-
	Before cure	1280.764	1280.718	-0.046	-46	-46
	After cure	1280.718	1271.57	-9.148	-9148	-9194

Angled beam No. 1 had a measured residual strain, after cure, of 1234 μin./in. Finite element analysis on the residual cure stress, shown in Figure 25, of an identical beamwidth of similar layup shows a strain range of 685 to 1670 μin./in. with an average of 1208 μin./in. The measured residual strain value, via Bragg grating, corresponded very well to the theoretical value.

The results for angled beams No. 2 and No. 3 were quite different than that of angled beam No. 1. Angled beams No. 2 and No. 3 had residual strains of -9490 and -9194 μin./in. respectively. This excessively high residual strain was caused by bending of the sensor during the manufacturing process.

The thickness of angled beam No. 1 after the layup process was 0.315 in. The mold was manufactured with a cavity height of 0.250 in. Because of the large difference between the actual layup thickness and the expected cure thickness it was theorized that the embedded sensor would buckle within the composite due to the 65 mils of compaction that would occur during the cure cycle. To combat this potential problem the composite was hot debulked to 200°F and 100 psi. A 15 mil spacer was placed between the mold halves to prevent full compaction of the part. After the debulk cycle was completed, the sensor was embedded through the thickness of the beam and the part was autoclave cured. After a spectrometer reading was taken on the sensor in the cured part, the sensor pulled out of the composite during excessive handling. The point at which the sensor to resin matrix bond failed is unknown. It was thought that the hot debulk cycle may have limited the resin flow during the cure cycle to produce such a weak bond. To combat this, the final two beams were manufactured without the hot debulk step.

By eliminating the hot debulk step from the manufacturing process of beams No. 2 and No. 3, full resin flow during the cure cycle gave a strong sensor to resin matrix bond. Unfortunately the measured residual strain values of -9000 microstrain indicate buckling of the sensor within the composite structure due to the compaction of the composite. Upon cross sectioning of the angled beams it was found that the sensors had actually buckled within the composite thickness.

It is apparent that additional processing modifications are required in the angled beam manufacture to produce a strong bond without buckling the sensor. One potential solution is to hot debulk the beam with the sensor already embedded. If the pigtail was not sealed in the salt plug, the sensor and pigtail could move freely during the hot debulk (i.e. compaction) cycle which would eliminate any buckling while allowing the matrix resin to flow onto the sensor surface yielding a strong bond.

3.3 Task 3 - Requirements for a Residual Strain Measurement System

Preliminary discussions were held with NAVAir to define the Navy's requirements for a residual strain measurement system. The system is required to be generic in the manner with which it can effectively measure residual strain in parts of different sizes and geometries. It must be applicable with different prepreg systems.

The current technology developed by Foster-Miller should be applicable to composite components made from various prepreg materials including thermoset systems such as AS4/3501-6, AS4/977-3 and IM7/8551 as well as thermoplastic systems such as AS4/APC2 and IM7/KIIIB. The modified ultrasonic embedding technique has been successfully evaluated on a related SBIR Phase I program (Ultrasonically Assisted Z-Fiber Insertion), on AS4/3501-6, IM7/8551 and IM7/KIIIB. With little modification, the embedding technique can be used for AS4/APC2, AS4/977-3 or most other prepreg systems. Part size and geometry will only be

Figure 25. Finite element analysis on cure strains in the angled beam

limited by the complexity of the tooling necessary to encapsulate and protect the fiber optic pigtail during the cure cycle.

Contact was made with personnel from McDonnell Douglas Aerospace East to define potential applications for a residual strain sensing system within the airframe community. One potential application that intrigued McAir involved a low cost procedure for manufacturing C-section stiffeners (shown in Figure 26). McAir has assessed the process of manufacturing two C-section components by cutting a square section in half (Figure 27). They theorized that the residual stresses due to the machining process would render the parts unusable. However, if by using the Foster-Miller approach these stresses could be measured and controlled, this concept might be realizable.

Foster-Miller is in the process of completing an Air Force funded Phase I SBIR program to develop specialized Bragg grating sensors that will be used to measure strain distributions along the length of the sensor. All of the work to date with Bragg sensors has been on measuring the average strain across the grating length. It is apparent that the measurement of strain distributions through the thickness of composite parts would yield data that were previously not measurable. If this technology has achieved maturity at the time of the Phase II Navy program it could be incorporated into the manufactured sensor system.

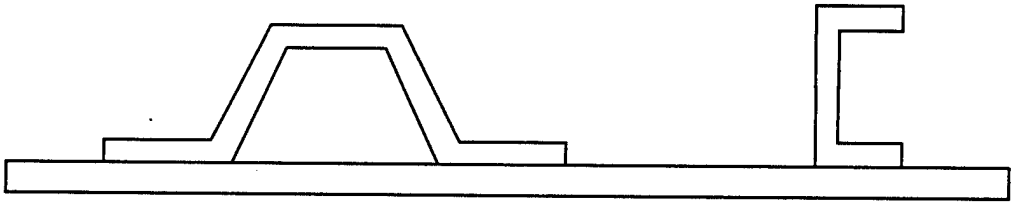

304-NAV-95046-2

Figure 26. C-section stiffeners

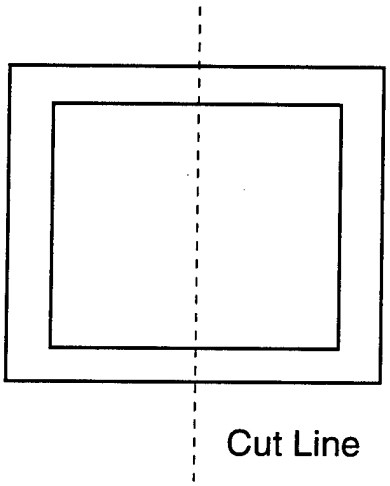

304-NAV-95046-3

Figure 27. Potential low cost manufacture of C-beams

4. CONCLUSIONS AND RECOMMENDATIONS

Foster-Miller has developed the basis for a through-thickness residual strain measurement system based on embedded Bragg grating technology. A modified ultrasonic process was devised to embed Bragg gratings through the thickness of uncured composite laminates. Novel tooling schemes were developed and built to protect the sensor during the cure cycle and to allow for the composite with embedded sensor to be removed without damaging the fiber optic. These tooling schemes allowed for up to three sensors to be embedded into each composite part and with proper design the number could be unlimited. Preliminary processing procedures were developed to ensure that the sensor consistently survived the setup, cure and demolding.

The ultrasonic embedding process, novel tooling scheme and processing procedures are applicable to most thermoset systems and some thermoplastic systems. The size and geometry of the composite part will only be limited by the complexity of the tooling required to encapsulate and protect the fiber optic pigtail during the cure cycle.

Two types of through thickness residual strain were measured: strain imparted into the composite by post cure cycle machining operations such as sectioning and drilling and strain due to thermal effects induced during the cure cycle. Residual strain due to post cure cycle machining operations was measured on flat plate composite components while an angled beam component served as the test article for the measurement of residual strain caused by the cure cycle.

Several cuts were made at various distances from the sensor locations. The sensor was able to measure strains when the cut was less than one laminate thickness, 0.250 in. in this case, away. Compressive strain changes no greater than 500 μin./in. were measured for cuts at 0.250 and 0.125 in. away from the sensor. On the one occasion when a closer cut was made, at 0.0625 in. away, the strain change was positive. In most cases the strain results were repeatable for the same sequence of cuts around different sensors.

Several drilled holes were machined at various distances away from the sensor locations. A compressive residual strain was measured for each 0.125 and 0.250 in. diameter hole drilled 0.250 in. away from the sensor. As in the sectioning experiment, when the hole was drilled closer to the sensor a positive strain change was measured due to crack propagation. The strain results for the identical sequence of drilled holes around different sensors were repeatable. On the average drilling was found to produce higher amounts of residual strain at the same free edge distance to the sensor than sectioning.

The preliminary task of the program showed that through-thickness strains due to machining operations could be measured with repeatable results. One suggestion for follow-on work would be to define a method to measure or calculate the expected residual strain due to machining in order to prove the validity of the strain measurements yielded by the Bragg gratings.

An angled beam representative of an F-18 humpback skin served as the composite component used to evaluate residual strain due to thermal effects caused by the cure cycle. A through-thickness residual strain of -1234 μin./in. was measured for one component. This

strain value correlates well to a finite element analysis on an identical angled beam with a similar layup that predicted -1208 μin./in. of residual strain. Two other beams yielded excessively high results. It was found that the sensors within these specimens buckled within the composite during the cure cycle. Additional work is required to refine the processing steps to eliminate this problem. One solution may be to hot debulk the part prior to the embedding process.

The Phase I program has verified the residual strain sensing capability of embedded through-thickness Bragg rating sensors. Continued work must correlate theoretical strain predictions with those measured. The current sensor technology, used in the Phase I program, measures average strain along the sensor. Most residual strains exhibit non-linear strain distributions, as well as discrete strain changes at each ply. Current work being conducted by Foster-Miller is demonstrating the ability to measure strain gradients along the sensor. This capability should be expanded to more accurately measure peak residual strains. Residual strain sensing on actual components using production tooling should also be conducted.